DOI: 10.1002/adsc.200600312

A Density Functional Theory Study of the Stille Cross-Coupling *via* Associative Transmetalation. The Role of Ligands and Coordinating Solvents

Rosana Álvarez,*[a] Olalla Nieto Faza,[a] Angel R. de Lera,[a,*] and Diego J. Cárdenas[b]

[a] Departamento de Química Orgánica, Facultade de Química, Universidade de Vigo, Lagoas-Marcosende s/n, 36310 Vigo, Spain
Phone: (+34)-986-812-316; fax: (+34)-986-811-940; e-mail: rar@uvigo.es or qolera@uvigo.es
[b] Departamento de Química Orgánica, Facultad de Ciencias, Universidad Autónoma de Madrid, 28049 Madrid, Spain

Received: June 28, 2006

Supporting information for this article is available on the WWW under http://asc.wiley-vch.de/home/.

Abstract: An associative mechanism has been computationally characterized for the Stille cross-coupling of vinyl bromide and trimethylvinylstannane catalyzed by PdL_2 (L = PMe_3, $AsMe_3$) with or without dimethylformamide as coordinating ligand. All the species along the catalytic cycles that start from both the *cis*- and the *trans*-PdL(Y)(vinyl)Br complexes (Y = L or S; L = PMe_3, $AsMe_3$ or PH_3; S = DMF) have been located in the gas phase and in the presence of polar solvents. Computations support the central role of species *trans*-PdL(DMF)(vinyl)Br which react by ligand dissociation and stannane coordination in the rate-limiting transmetalation step *via* a puckered four-coordinate (at palladium) transition state comprised of Pd, Br, Sn and sp^2 C atoms. A donating solvent may enter the catalytic cycle assisting isomerization of *cis*-PdL_2(vinyl)Br to *trans*-PdL(DMF)(vinyl)Br complexes *via* a pentacoordinate square pyramidal Pd intermediate. In keeping with experimental observations, the activation energies of the catalytic cycles with arsines as Pd ligands are lower than those with phosphines. Polytopal rearrangements from the three-coordinate T-shaped Pd complexes resulting from transmetalation account for the isomerization and the C–C bond formation on the reductive elimination step.

Keywords: associative mechanism; catalysis; cross-coupling; DFT study; palladium; Stille reaction

Introduction

The impact that metal-catalyzed cross-coupling processes,[1] in particular the Stille and the Suzuki reactions, have on synthesis is unquestioned. High selectivity, functional group tolerance and mildness of the reaction conditions make these processes a sensible choice for C–C bond formation even in the complex setting of natural product synthesis.[2] On reviewing the current knowledge of the Stille reaction,[3] Espinet and Echavarren recognized that the variation in reaction conditions (i.e., additives, solvents, halides/pseudohalides, palladium source, ligands, the "copper cocatalysis", etc.) employed by most practitioners for this cross-coupling are still rather empirical. Clearly, the classical texbook cycle, comprising the oxidative addition, transmetalation and reductive elimination steps (Figure 1), although accounting for the overall transformation and for the catalytic role of the transi-

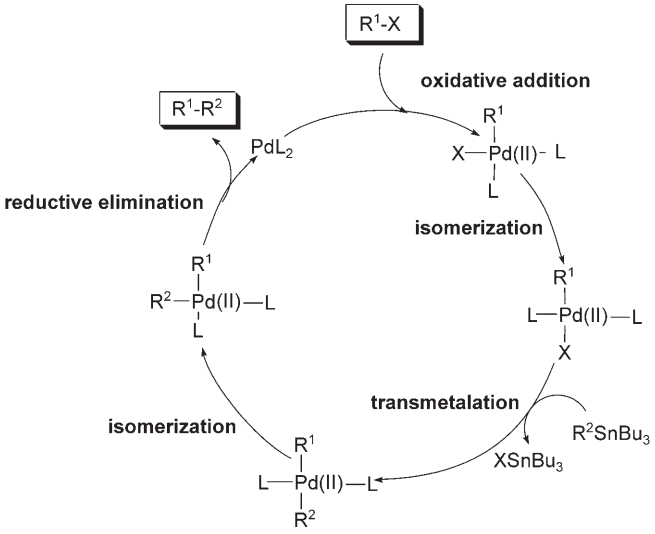

Figure 1. Simplified mechanistic depiction of the Stille cross-coupling reaction under catalysis of palladium complexes with monodentate ligands.

tion metal, fails to provide structural and geometrical details of the different structures involved as intermediates or transition states. Accumulating kinetic and stereochemical knowledge prompted the emergence of multifaceted reaction mechanisms in place of the simplified and familiar texbook display.

Being part of other transition metal-catalyzed transformations, the oxidative addition and the reductive elimination steps are reasonably well understood and experimental as well as computational studies abound in the literature.[4] Yet, the geometric requirements for these elementary steps, which are oftentimes ignored, demand the incorporation to the cycle of additional isomerization steps involving the *cis*- and *trans*-square planar complexes at palladium (Figure 1). Regardless of the importance of these geometric changes, it is clearly in the transmetalation step where significant mechanistic variations are expected depending upon the so-called nucleophilic component (organoborane, organostannane, organozinc, Grignard reagent etc.), giving rise to the subtlities of the different versions of the cross-coupling processes (Suzuki, Stille, Negishi, Kumada etc) that are beginning to emerge.[1]

Pioneering studies by Farina et al. on the role of palladium ligands showed that the reaction of organic halides and stannanes followed a kinetic law with first-order dependence on [Sn] and [Pd] and inverse first-order dependence on [L].[5] A dissociative pre-equilibrium of $PdL_2(R^1)X$ to $L+PdL(R^1)X$ or its solvent-stabilized derivative $PdL(S)(R^1)X$ was proposed to explain the retarding effect of the free ligand. In particular, triphenylphosphine was identified as a powerful inhibitor of the transmetalation step. This observation led to the evaluation of ligands of lower donicity [$AsPh_3$, $(o\text{-furyl})_3P$] that were found to accelerate the Stille coupling by a factor of up to 10^2 relative to PPh_3. It was early hypothesized that the much larger pre-equilibrium concentration of the solvato complex $PdL(S)(R^1)X$ accelerates the transmetalation.[5]

Insights into the kinetic rate law in the Stille coupling of aryl triflates and tributylvinylstannane,[6] and reflections on the previously known and puzzling evidence that retention of configuration occurs with some chiral non-racemic hydroxyalkylstannanes,[7] led Casado and Espinet to postulate two mechanisms for the transmetalation step of the Stille reaction, termed *cyclic* and *open* (Figure 2).[8]

The S_E(open) mechanism implies the dissociation of the anionic ligand X, and therefore appears to be restricted to non-bridging X ligands (pseudohalides such as triflates) in particular in the presence of polar, coordinating, non-bridging solvents. The overall result is the replacement of X (or L, if the former dissociates) for R^2 at palladium. α-Chiral non-racemic alkylstannanes should couple to electrophiles with inversion of configuration occurring at this stage [see **TS(B)** in Figure 2].

The associative mechanism was considered to be favored for the coupling of X bridging electrophiles and stannanes. The replacement of L for R^2 [see **TS(A)** in Figure 2], with retention of configuration for the same α-chiral R^2 groups, should in turn proceed

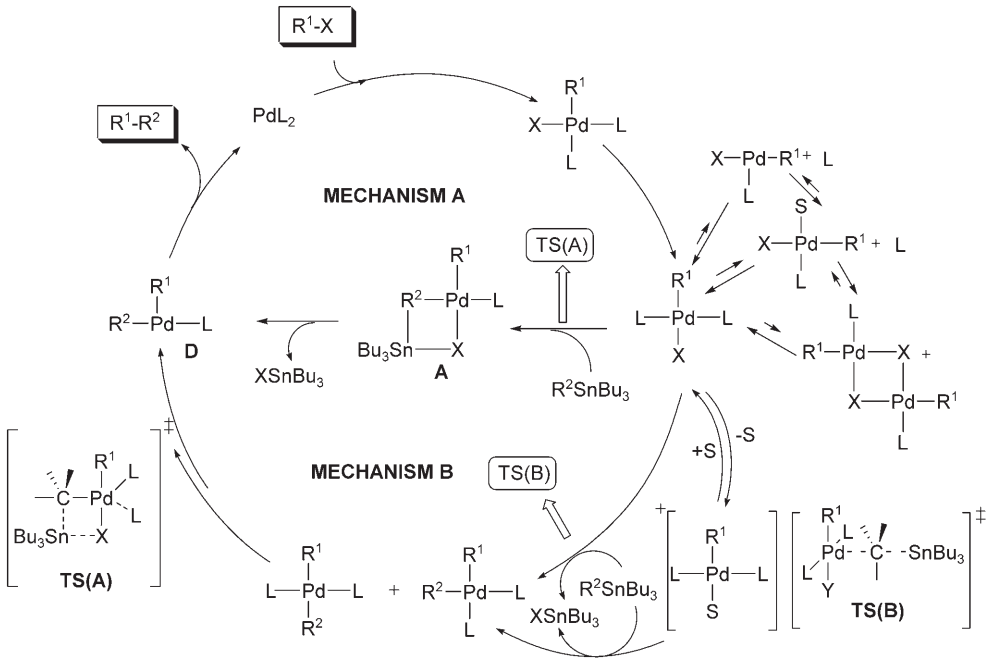

Figure 2. Competing associative and dissociative catalytic cycles proposed by Casado and Espinet for the Stille cross-coupling reaction (adapted from ref.[8]).

through a cyclic transition state (or intermediate). An attractive feature of this proposal resides in the *cis* geometric arrangement of the carbon ligands at palladium after transmetalation (structure **D** in Figure 2). The ensuing reductive elimination, although it is assumed to be very fast in most settings, would not require additional isomerization steps.

The description of complex mechanistic proposals, such as the catalytic cycles promoted by substoichiometric quantities of transition metals, greatly benefits from the current power of computational chemistry. Recent reports in C–C coupling reactions have evaluated different aspects of the Suzuki–Miyaura reaction, such as the role of the base adding to the organoboronic acid rather than to palladium,[9] the coupling of aryl halides with a diboron species[10] and that of carboxylic anhydrides with arylboronic acids.[11] Given the difficulties in the isolation and characterization of the proposed (and unexpected) intermediates, computational chemistry is shedding some light into the structural and energetic details of some of these relevant C–C bond-forming processes.[12]

We have recently reported[13] a DFT study supporting the cyclic transmetalation mechanism in the Stille coupling and characterized an associative ligand substitution mechanism as well as a cyclic species as the highest-energy transition state in the complete catalytic cycle (mechanism **A** in Figure 2). As a model reaction we studied the coupling of vinyl bromide **1** and trimethylvinylstannane **2** catalyzed by $Pd(PMe_3)_2$/PMe_3 (Figure 3) in the gas phase and in a polar solvent using density functional theory[14] calculations. We also considered the role of a coordinating solvent (DMF) as explicit palladium ligand, and depicted a catalytic associative mechanism involving the Pd(L)(Y)(vinyl)Br complex that competes favorably with that of $Pd(PMe_3)_2$(vinyl)Br species. We computed a smaller activation energy for the solvato complex on the rate-determining transmetalation step. In addition, the coordinating solvent also favors

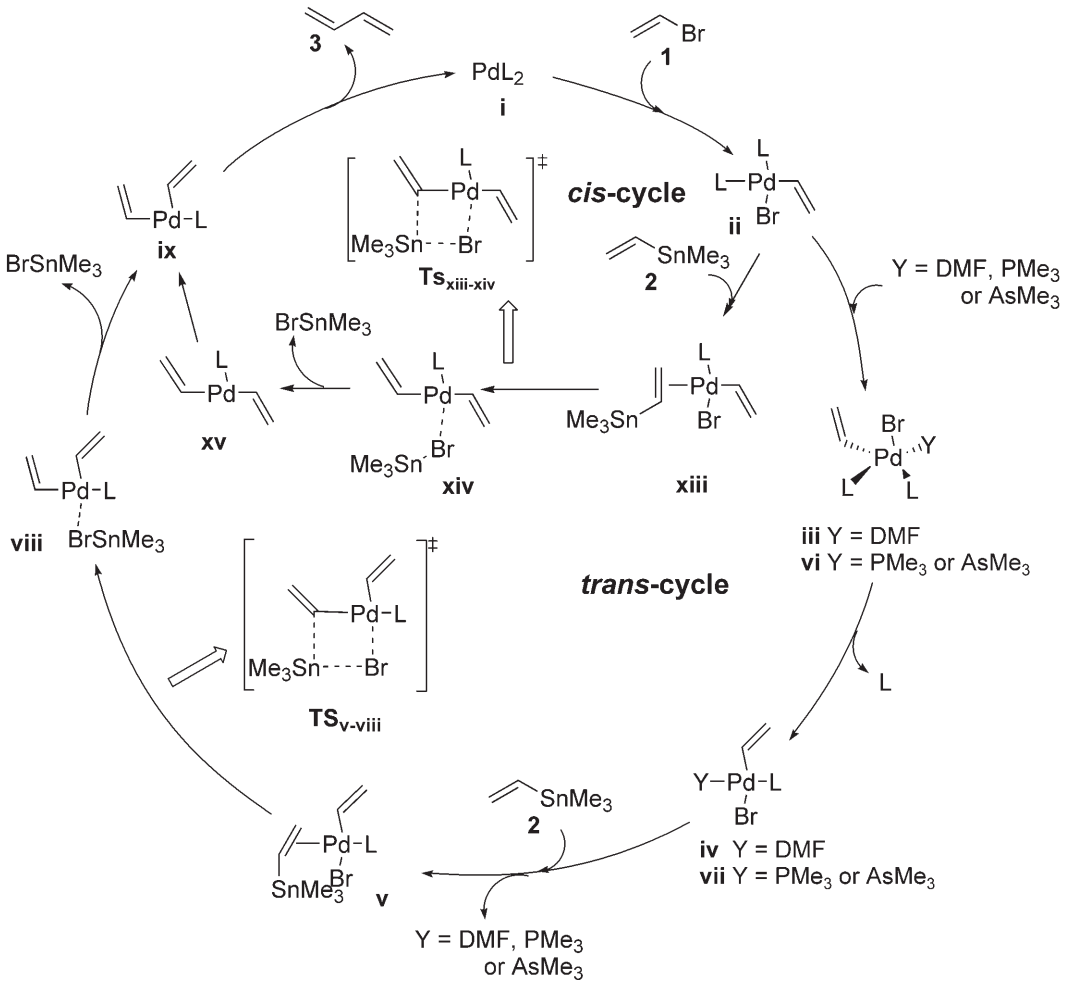

Figure 3. Catalytic cycle for the associative Stille cross-coupling reaction between vinyl bromide **1** and trimethylvinylstannane **2** through a cyclic transmetalation transition state, starting from the *trans*- or the *cis*-Pd(L)(Y)(vinyl)Br complexes (Y = PMe_3, $AsMe_3$, DMF).

the *cis-trans* isomerization, which we showed to be feasible *via* pentacoordinate palladium complexes formed by ligand (L or S) association after oxidative addition.

The incorporation of coordinating solvent ligands was justified by the need to understand the puzzling reports on the effect of solvent in Stille coupling reactions.[5,15,16] Following the pioneering findings of Farina and Krishnan,[5] Amatore and Jutand disclosed through detailed kinetic studies contrasting effects of the solvent depending upon the timing of the oxidative addition step. On the one hand, a retarding effect was seen if the tributylvinylstannane nucleophile coordinates to a $Pd(AsPh_3)_2(S)$ complex formed prior to the oxidative addition to Ph–I. The formation of a η^2-$[CH_2{=}CH\text{-}Sn(n\text{-}Bu)_3]Pd(AsPh_3)_2$ species is a side reaction that stores part of the catalyst load under an unreactive form. On the other hand, if the complex $Pd(AsPh_3)_2(Ph)I$ is formed upon oxidative addition, it dissociates one $AsPh_3$ molecule in DMF and $CHCl_3$, with concomitant formation of a new Pd(II) moiety ligated by only one $AsPh_3$, which was assigned to be the $Pd(AsPh_3)(S)(Ph)I$ complex.[15] Whereas in THF the relevance of this complex is unlikely,[8] the kinetics of the transmetalation step established that $Pd(AsPh_3)(DMF)(Ph)I$ is the actual species that reacts with $CH_2{=}CH\text{-}Sn(n\text{-}Bu)_3$.[16]

We report herein a full account of this work, summarized in the mechanistic manifold depicted in Figure 3, which further supports the cyclic associative transmetalation mechanism proposed for alkenyl halides.[8] For completion, we have also included the study of the transmetalation step starting from the *cis*-PdL_2(vinyl)Br oxidative addition intermediates. The following interconnected aims will be addressed: a) the comparison between PMe_3 and $AsMe_3$, as representative models of donating and dissociative ligands; b) the similarities and differences between PMe_3 and PH_3 as model palladium ligands having different electron donicity and steric influence; c) the relevance of a coordinating solvent (DMF) molecule acting as a palladium ligand upon replacement of a phosphine or arsine; d) the comparison between two possible transmetalation mechanisms, starting from the *cis* and *trans* isomers of the PdL_2(vinyl)Br complex; e) the analysis of the evolution of a three-coordinated species formed upon transmetalation *via* the cyclic associative mechanism; f) the description of the reductive elimination step; g) the evaluation of the reaction energies in solvent (THF, CH_3CN) using continuum models.

Results

With the main focus on the analysis of the alternative rate-limiting transmetalation paths, the results will be presented according to the general steps of the Stille catalytic cycle. Along the discussion, since these reaction variants share some of the intermediates, the activation energies will be compared. An overall potential energy surface plot along the reaction coordinate for the entire Stille catalytic cycle will be presented in the discussion section.

The Oxidative Addition

Recent experimental[17] and computational[18] studies on the oxidative addition of aryl halides to Pd(0) complexes concur that the initial species is a square planar d^8 *cis*-Pd(II) complex. For alkenyl bromides, we also confirmed these findings (Figure 4), and the starting 14-e$^-$ species PdL_2 **i** is converted into the square-planar 16-e$^-$ complex *cis*-PdL_2(vinyl)Br (L = $AsMe_3$, **ii.As**; L = PMe_3, **ii.P**) with a large energy barrier (18.9 kcal mol^{-1} for **ii.P**; 16.2 kcal mol^{-1} for **ii.As**). Vinyl bromide **1** coordinates first to PdL_2 by means of the double bond through a η^2 complex,[19] and oxidative addition takes place *via* the three-center transition state $\mathbf{TS_{i\text{-}ii}}$**.P**. The main geometric features of $\mathbf{TS_{i\text{-}ii}}$**.P** (Figure 5) are the distances between Pd and the unsaturated carbon atoms of 1.90 (proximal) and 2.40 Å (distal) (1.99 and 2.61 Å for $\mathbf{TS_{i\text{-}ii}}$**.As**), and the bond distances of Br to Pd and C of 2.88 and 2.49 Å (2.83 and 2.45 Å for $\mathbf{TS_{i\text{-}ii}}$**.As**). Square-planar *cis*-PdL_2(vinyl)Br complex **ii**, having a *cis* arrangement of the entering groups is then formed, in a concerted overall exergonic process (the Gibbs free energy difference between **i** and **ii** is 9.7 kcal mol^{-1} for L = PMe_3 and 10.9 kcal mol^{-1} for L = $AsMe_3$). These *cis* complexes have been historically neglected since in most cases only the intermediates $PdL_2(R^1)X$ with *trans* configuration had been observed in Stille reactions. This view is, however, challenged mechanistically [the three-center transition state should lead to *cis*-$PdL_2(R^1)X$ rather than to *trans*-$PdL_2(R^1)X$], experimentally (NMR detection,[17a,20]) and computationally,[18] as stated above. Nevertheless, *cis*-$PdL_2(R^1)X$ complexes are relevant for Stille coupling reactions that use chelating diphosphines, and have been occasionally characterized.[21]

The presence of solvent molecules (either CH_3CN or THF; only the results for the former are included in the text, but those in THF are comparable, and are listed in the Tables) stabilizes all structures, in particular the transition state $\mathbf{TS_{i\text{-}ii}}$ (Figure 4; Table 1). This stabilization is greater for the complexes having $AsMe_3$ rather than PMe_3 as palladium ligands (4.9 kcal mol^{-1} *vs.* 2.4 kcal mol^{-1}), providing a substantial reduction in the activation energy (2.5 kcal mol^{-1} lower for $AsMe_3$ than for PMe_3) for the concerted insertion of palladium into the C–Br bond when bound to an arsine relative to phosphine in solution (the ac-

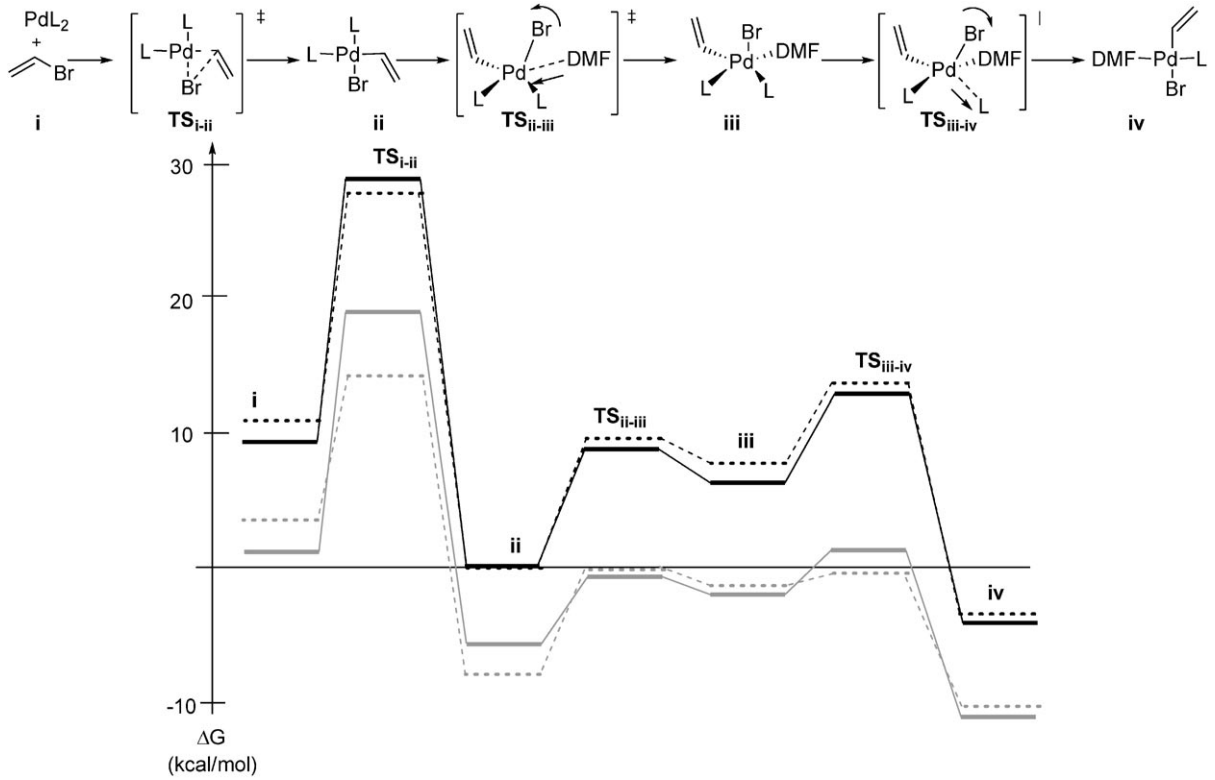

Figure 4. The oxidative addition of vinyl bromide **1** to the 14 e^- PdL_2 complex to form *cis*-PdL_2(vinyl)Br **ii** and its isomerization to the *trans* product [*trans*-PdL_2(vinyl)Br] **iv** assisted by DMF as ligand (solid line, L = PMe_3; dotted line, L = $AsMe_3$; black, gas phase; grey, CH_3CN-COSMO).

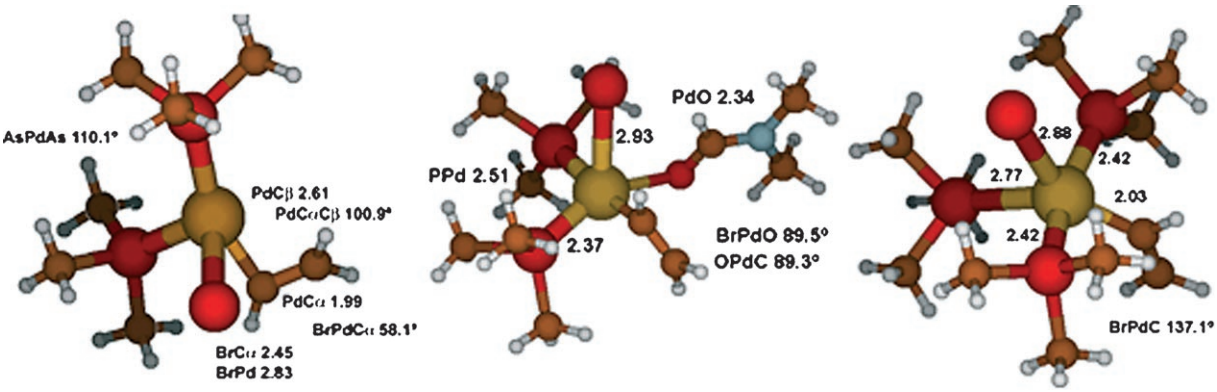

Figure 5. Optimized geometries (B3LYP/6-31G*-SDD) for the transition structures **$TS_{i\text{-}ii}$-As**, **$TS_{ii\text{-}iii}$-As** and **$TS_{vi\text{-}vii}$-As** characterized in the oxidative addition of vinyl bromide to PdL_2 and the *cis-trans* isomerization of *cis*-PdL_2(vinyl)Br (Figure 4).

tivation energies in CH_3CN are 11.3 and 16.5 kcal mol^{-1}, respectively).

The *cis-trans* Isomerization

Following the classical catalytic cycle, *cis*-PdL_2(vinyl)Br complex **ii** undergoes isomerization to *trans*-PdL_2(vinyl)Br prior to transmetalation. Three different mechanisms are usually considered for *cis-trans* isomerization in square planar complexes: the usual two-step associative pathway,[22] the associative pathway with Berry pseudorotation prior to ligand dissociation from the 18-e^- complex[23] and the dissociative pathway.[24] The nature of the solvent, the ligands and the temperature are the main factors affecting the isomerization mechanism and its rate. Previous kinetic analysis[20] revealed that the *cis-trans* isomerization of complexes of certain aryl iodides and $Pd(PPh_3)_4$ proceeds *via* five major parallel pathways. The two of

Table 1. Gibbs free energies (in kcal mol^{-1}) for the oxidative addition and *cis-trans* isomerization steps depicted in Figure 4 and Figure 6. The values are given relative to the *cis* square planar complex **ii** in gas phase.

Structure	$L=PMe_3$			$L=AsMe_3$		
	$\Delta G^{[a]}$	$\Delta G^{[b]}$	$\Delta G^{[c]}$	$\Delta G^{[a]}$	$\Delta G^{[b]}$	$\Delta G^{[c]}$
i+1	9.7	1.6	−1.1	10.9	3.4	6.8
TS_{i-ii}	28.6	18.1	17.4	27.1	14.7	18.8
ii	0.0	−4.9	−0.4	0.0	−7.1	−2.9
TS_{iiii}	8.0	−0.5	−1.9	8.5	−1.8	3.5
iii	6.9	−1.1	−2.5	7.5	−2.1	3.2
TS_{iii-iv}	12.5	1.1	−0.2	12.8	−0.04	5.3
iv	−4.7	−11.5	−5.3	−4.5	−10.1	−5.4
TS_{iivi}	15.4	3.4	10.4	11.7	−3.2	1.8
vi	10.2	1.1	6.6	7.7	−3.5	1.4
TS_{vi-vii}	9.4	−2.0	3.3	8.5	−8.3	−3.3
vii	−11.3	−20.8	−16.2	−10.3	−21.3	−17.2
TS_{vii-v}	19.1	−1.8	4.0	16.5	−6.6	−1.2

[a] Gas phase.
[b] CH_3CN (COSMO).
[c] THF (COSMO).

lower energy involve bimolecular mono-iodo bridged complexes generated by a direct or a solvent-assisted replacement of phosphine by an iodo ligand of another complex. Two other mechanisms proceed through Berry pseudorotations on pentacoordinated species. The last mechanism involves an intramolecular rearrangement by mediation of a tetrahedral transition state that can be viewed as a rotation around the palladium center. Despite our efforts and experience in the field,[25] we were unable to locate transition structures corresponding to Berry pseudorotations and tetrahedral species. The mechanisms of the dimeric complexes are beyond computational feasibility at present. Nevertheless, a plausible alternative would simply imply the excess ligand (Figure 6) or solvent-assisted (Figure 4) isomerization of monomers in reactions run in the presence of coordinating solvent. The alternative paths linking intermediates **ii** and **iv** or **vii** are depicted in Figure 4 and Figure 6, respectively.

We found that both the solvent- and the ligand-assisted topomerizations of **ii** into **iv** or **vii** take place through pentacoordinate complexes of rather low energy (Figure 4 and Figure 6). These $PdL_2(Y)$-(vinyl)Br intermediates (Y = DMF, **iii**; Y = L, **vi**) show square-planar pyramidal geometries with bromide occupying the axial position, stabilizing the complex along the *z*-axis where the electron density is lower, by electrostatic interaction (Figure 7).[26] Both structures, **iii** and **vi**, are geometrically similar, with Pd−Br distances of 3.30 and 3.10 Å for **iii** and **vi**, respectively, when $L=PMe_3$ (3.29 Å for **iii** and 3.10 Å for **vi** when $L=AsMe_3$). The *trans*-square planar complexes **iv** and **vii** are formed by *trans*-ligand release from the transition structures **TS_{vi-vii}** (Figure 5) and **TS_{iii-iv}**.[27]

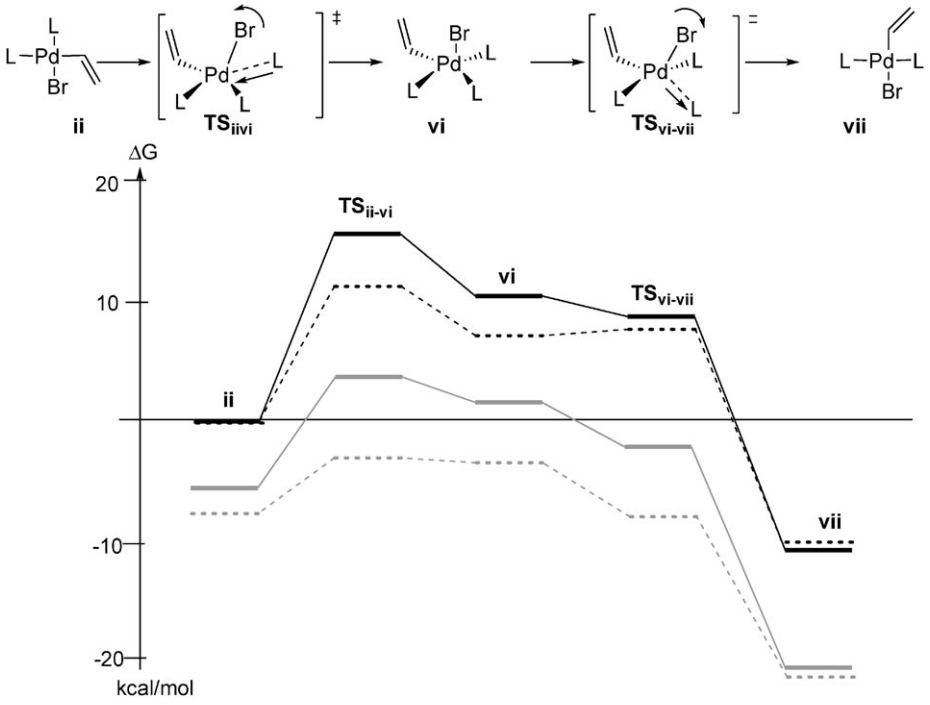

Figure 6. The isomerization of *cis*-PdL_2(vinyl)Br **ii** to the *trans* product [*trans*-PdL_2(vinyl)Br **vii**] assisted by $AsMe_3$ or PMe_3 in an associative ligand substitution process (solid line, $L=PMe_3$; dotted line, $L=AsMe_3$; black, gas phase; grey, CH_3CN-COSMO).

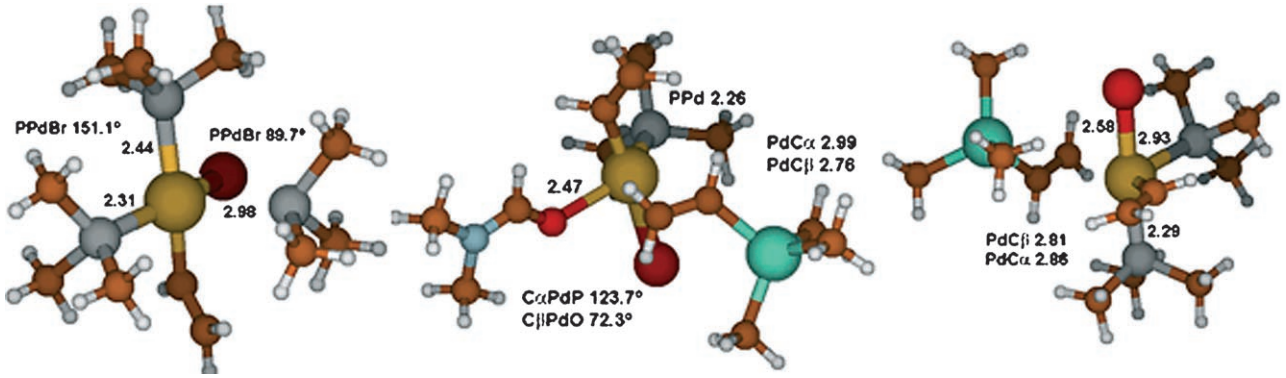

Figure 7. Optimized geometries (B3LYP/6-31G*-SDD) for the transition states $\mathbf{TS_{ii\text{-}vi}}$, $\mathbf{TS_{iv\text{-}v}}$ and $\mathbf{Ts_{ii\text{-}xiii}}$ with PMe_3

Despite their similarity, it is striking that the transition state $\mathbf{TS_{iii\text{-}iv}}$ with mixed ligands (DMF and PMe_3/$AsMe_3$) is located 5.5 kcal mol^{-1} above **iii.P** (5.3 kcal mol^{-1} for **iii.As**) whereas the corresponding analogue with identical ligands $\mathbf{TS_{vi\text{-}vii}}$ is found downhill along the coordinate leading to the *trans* complex **vii**. The overall *cis-trans* isomerization process is exergonic (4.7 kcal mol^{-1} for **ii.P–iv.P**; 11.3 kcal mol^{-1} for **ii.P–vii.P**; 4.5 kcal mol^{-1} for **ii.As–iv.As**; 10.3 kcal mol^{-1} for **ii.As–vii.As**). The isomerization path *via* the solvent associative addition that exchanges a PMe_3 or $AsMe_3$ by DMF leads to intermediate *trans*-PdL(DMF)(vinyl)Br **iv** with higher electrophilicity for subsequent attachment of the stannane nucleophile.

A polar solvent stabilizes all intermediates and transition structures, and therefore the overall effect in reaction barriers is modest. Along the path from the *cis* to the *trans* complexes assisted by DMF, there is a non-systematic effect of solvent for either PMe_3 or $AsMe_3$. When comparing both isomerization paths, the *trans* intermediates **iv** are of higher energy than **vii**. The destabilization of **iv** together with its greater electrophilicity will cooperate to provide a reaction path of lower energy for the solvato complex in the rate-determining transmetalation (*vide infra*).

According to the computed activation energies, it is concluded that the *cis-trans* isomerization occurs at a very fast rate relative to oxidative addition and transmetalation. Activation energies range from 3.9 kcal mol^{-1} for $AsMe_3$-assisted isomerization to 9.0 kcal mol^{-1} for the PMe_3-assisted isomerization (in CH_3CN solution), those assisted by DMF being of intermediate value (around 5 kcal mol^{-1}) regardless of the ligand used (Table 1).

The Transmetalation

The low polarity of the Sn–C bond distinguishes the Stille reaction from other organometallic processes using more polar partners (e.g., Grignard reagents in the Kumada reaction) and that property should manifest itself on the transmetalation, the step commonly considered to be rate-determining.

Two mechanisms have been recently suggested[3] for the transmetalation step.[8] **Pathway A** involves a ligand substitution on a Pd complex through a 14-electron T-shaped intermediate (*dissociative substitution X-for-R^2*). **Pathway B** goes through an 18-electron trigonal bipyramidal complex as an intermediate or transition state and, often, includes as variants a *direct substitution* and a *solvent-assisted substitution* (*associative substitution L-for-R^2 or Y-for-R^2*). Both variants can, moreover, proceed through a cyclic or an open transition state.[13b] Herein, we consider for computational purposes the mechanism that involves the *L-for-R^2* substitution (**Pathway B**), the most favored for the coupling of organic halides as electrophiles and stannanes as nucleophiles. Since the oxidative addition intermediate forms with *cis* geometry, we studied both transmetalation processes taking place from the complexes differing in ligand arrangement around palladium.

Pathway from the *trans*-Square Planar Complex (*trans*-PdL_2R^1X)

Casado and Espinet envisioned an *L-for-R^2* S_E-transmetalation at the Pd center with X ligands capable of acting as bridging groups in which ligand substitution and formation of a cyclic species occur in concert *via* a five-coordinate transition state (or intermediate) at Pd.[8] However, at least for alkenylstannanes, our computations support a stepwise process in which associative ligand substitution precedes the formation of a cyclic transition state (Figure 8). In the first stage, the double bond of trimethylvinylstannane **2** coordinates to the Pd complex (η^2-coordination), facilitating dissociation of the ligand or the solvent *via* a transition state ($\mathbf{TS_{iv\text{-}v}}$ and $\mathbf{TS_{vii\text{-}v}}$) with a geometry that shows features of a trigonal bipyramid (Figure 7). The apical positions are occupied by the bromide (Pd–Br bond distances: for L = PMe_3, 2.62 for $\mathbf{Ts_{iv\text{-}v}}$ and

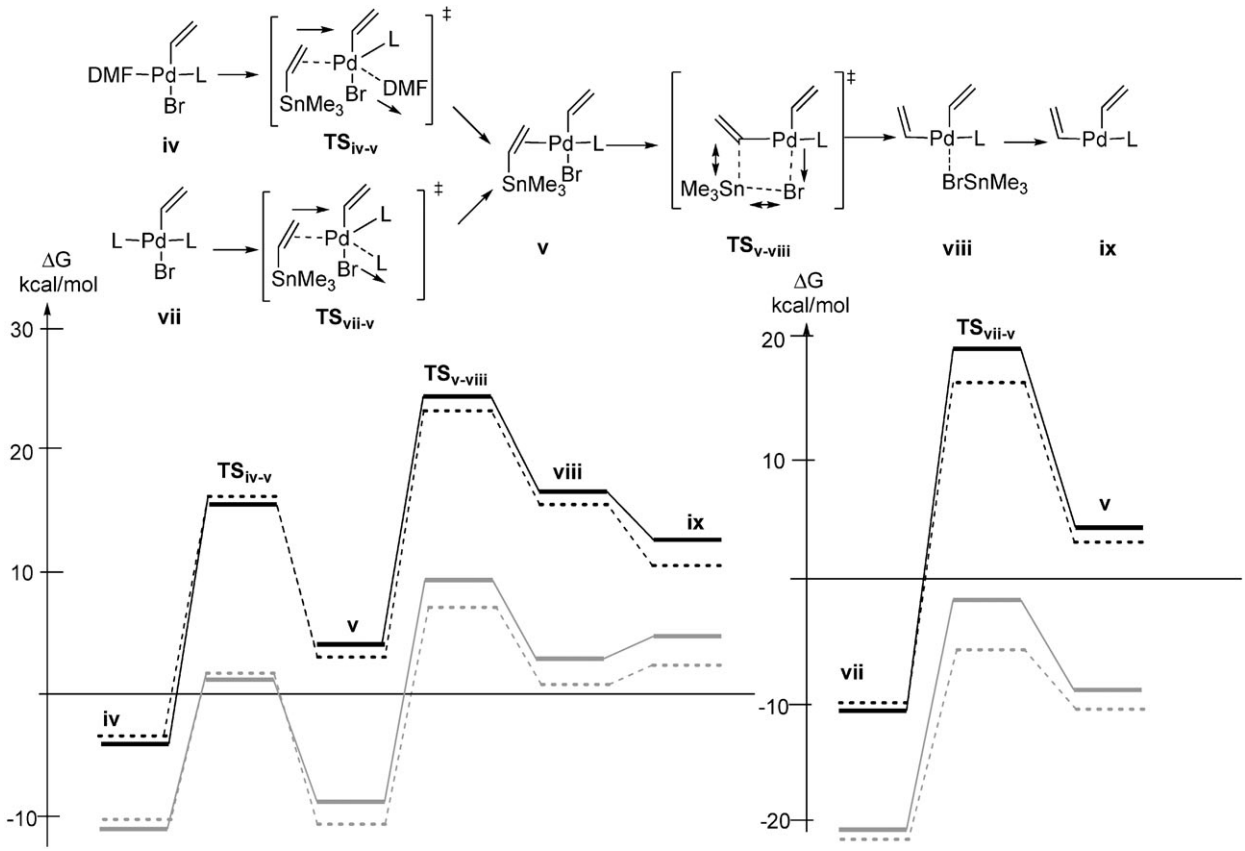

Figure 8. The transmetalation mechanism starting from the *trans*-PdL(DMF)(vinyl)Br **iv** (left) and *trans* PdL_2(vinyl)Br (right) **vii** complexes (solid line, L = PMe_3; dotted line, L = $AsMe_3$; black, gas phase; grey, CH_3CN-COSMO)

2.88 Å for **Ts$_{vii-v}$**, respectively; for L = $AsMe_3$, 2.63 and 2.65 Å, respectively) and vinyl substituents.

Coordination of stannane **2** to the Pd complexes **iv** and **vii** is against an energy barrier of 20.4 and 30.4 kcal mol^{-1} for L = PMe_3, respectively (20.6 and 26.8 kcal mol^{-1} for L = $AsMe_3$, respectively), whereas the energy difference between **iv** or **vii** and **v** amounts to 9.0 and 15.6 kcal mol^{-1}, respectively, for L = PMe_3 (7.5 and 13.3 kcal mol^{-1}, respectively, for L = $AsMe_3$). Table 2 lists the free energy values for the minima and saddle points characterized along the transmetalation step.

In order to gauge the influence of the phosphine ligand, we also computed the energetics of the transmetalation mechanism for the simplest PH_3. In constrast to PMe_3 and $AsMe_3$, association of the stannane to **vii.PH$_3$** occurs without concomitant ligand release, through **Ts$_{vii-x}$.PH$_3$** and requires 17.8 kcal mol^{-1} (Table 3). This behavior signals an important role of the ligand steric effects in the formation of the transition states and intermediates with pentacoordinate geometry at palladium. Furthermore, a bipyramidal complex **x.PH$_3$** has been located as a minimum for Pd coordinated to PH_3. Geometries of the transition states **TS$_{vii-v}$.P** and **TS$_{vii-x}$.PH$_3$** are roughly similar regardless of the ligand, and **TS$_{vii-x}$.PH$_3$** also adopts a trigonal bipyramidal geometry in which the apical positions are occupied by the bromide (Pd–Br bond distance of 2.66 Å) and vinyl (Pd-vinyl bond distance of 2.01 Å) substituents.

All structures listed on Table 3 are stabilized in THF and CH_3CN, and this translates into an energy of activation in solution of 9.3 kcal mol^{-1} for CH_3CN

Table 2. Gibbs free energies (in kcal mol^{-1}) for the species located on the transmetalation mechanism depicted in Figure 8. The values are given relative to the oxidative addition *cis*-complex *cis*-PdL_2(vinyl)Br **ii**.

Structure	L = PMe_3			L = $AsMe_3$		
	ΔG[a]	ΔG[b]	ΔG[c]	ΔG[a]	ΔG[b]	ΔG[c]
iv	−4.7	−11.5	−5.3	−4.5	−10.1	−5.4
TS$_{iv-v}$	15.6	0.7	6.8	16.1	0.8	6.8
v	4.3	−9.1	−4.3	3.0	−11.2	−6.6
TS$_{v-viii}$	24.7	9.6	14.3	23.0	7.1	11.7
viii	17.1	2.3	7.3	15.7	0.1	4.8
ix	12.6	4.9	4.3	10.7	2.3	5.4
vii	−11.3	−20.8	−16.2	−10.3	−21.3	−17.2
TS$_{vii-v}$	19.1	−1.8	4.0	16.5	−6.6	-1.2

[a] Gas phase.
[b] CH_3CN (COSMO).
[c] THF (COSMO).

Table 3. Gibbs free energies (in kcal mol^{-1}) for the coordination of trimethylvinylstannane **2** to *trans*-Pd$(PH_3)_2$(vinyl)Br **vii.PH$_3$**.

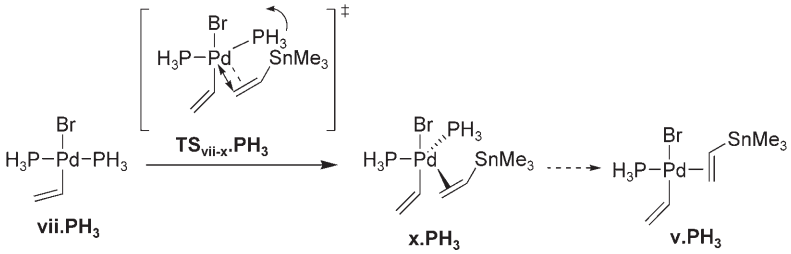

Structure	$\Delta G^{[a]}$	$\Delta G^{[b]}$	$\Delta G^{[c]}$
vii.PH$_3$	0.0	−2.8	0.4
TS$_{vii\text{-}x}$.PH$_3$	17.8	6.4	11.1
x.PH$_3$	16.7	5.5	10.2

[a] Gas phase.
[b] CH_3CN (COSMO).
[c] THF (COSMO).

(11.1 kcal mol^{-1} for THF), which is about 10 kcal mol^{-1} smaller that those measured for bulkier ligands (*cf.* L = PMe_3, 19.0 kcal mol^{-1} in CH_3CN and 20.2 kcal mol^{-1} in THF; L = $AsMe_3$, 14.7 kcal mol^{-1} in CH_3CN and 15.9 kcal mol^{-1} in THF for the pathway between **vii** and **v**). These energy differences indicate that changing substituents on phosphorus can induce marked changes in the properties and reactivities of the transition metal complexes in which they participate.[28]

Despite our efforts, a pentacoordinated transition state or intermediate at Pd (for either L = PMe_3 or $AsMe_3$) with a halogen atom bridging tin and palladium in a four-membered ring [**TS(A)** in Figure 2] could not be located. Among other modifications, we explored the transition structures for the series of halogens (Cl, Br, I) with restrained distances and angles for the key bonds. However, as soon as restrictions were removed, the ring opened up and the dihedral flipped, keeping a X-----Sn distance that increased with the size of the halogen. Moreover, adding a ligand to palladium on **TS$_{v\text{-}viii}$** leads to unstable structures, an indication that Pd is reluctant to engage in bipyramidal geometries with two of the ligands in a four-membered ring.[29]

We were able instead to characterize a *cyclic four-coordinate* (at Pd) transition state **TS$_{v\text{-}viii}$** with a Br ligand bridging Sn and Pd. The Br–Pd, Br–Sn and C–$SnMe_3$ bond distances are 2.71, 2.79 and 3.23 Å, respectively, for L = PMe_3 (Figure 9) and similar values for L = $AsMe_3$ (2.71, 2.78 and 3.33 Å, respectively). Inspection of the normal mode associated with the unique imaginary frequency reveals that the Me_3Sn is shifting rapidly (or pivoting) between the vinyl and Br groups. A cyclic transition state was also found by Napolitano et al.[29] in their computational study of the Stille coupling between alkynyl groups using as model systems tetraethynylstannane and a *trans*-Pd-$(PH_3)_2$(ethyne)Br complex. As NH_3 was included as nucleophile, the favored pathways in these cases were

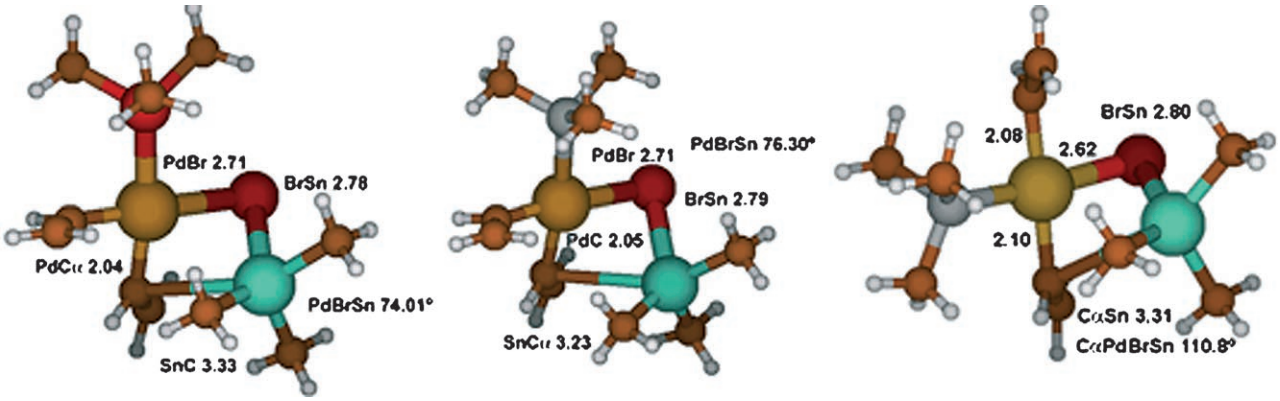

Figure 9. Optimized geometries (B3LYP/6-31G*-SDD) for the cyclic transmetalation transition states **TS$_{v\text{-}viii}$** with $AsMe_3$ and PMe_3 and **TS$_{xiii\text{-}xiv}$** with PMe_3 as palladium ligands.

computed to be the nucleophilically-assisted transmetalations from a hexacoordinated tin. Results from recent computations on aryl-vinyl Stille coupling are also in line with our findings.[13b]

As noted in Table 2 and Figure 8, the entire process from intermediate **iv** is endergonic; an energy difference between **v** and **viii** of 12.8 kcal mol^{-1} for L = PMe_3 (12.7 kcal mol^{-1} for L = $AsMe_3$) was computed. Reaching $\mathbf{TS_{v\text{-}viii}}$ from **v** requires the former to surmount an energy barrier of 20.4 kcal mol^{-1} for L = PMe_3 (20.0 kcal mol^{-1} for L = $AsMe_3$).

Thus, for vinyl partners, our computations identified a rate-limiting transmetalation step which involves the stepwise formation of the cyclic transition state with two consecutive barriers corresponding to the stannane coordination ($\mathbf{TS_{iv\text{-}v}}$ or $\mathbf{TS_{vii\text{-}v}}$) and the ligand or solvent release to afford **v** followed by formation of the four-atom transition state ($\mathbf{TS_{v\text{-}viii}}$). The overall activation barriers for transmetalation using PMe_3 ligand are 29.5 kcal mol^{-1} for Y = DMF, and 36.0 kcal mol^{-1} for Y = PMe_3. For analogues with $AsMe_3$ as ligand these values are smaller, 27.6 kcal mol^{-1} for Y = DMF, and 33.4 kcal mol^{-1} for Y = $AsMe_3$. With the incorporation of a solvent field in the computations, the energy profiles change and a reduction in activation energy values are noted, since all structures starting from **v** are stabilized in solution. Particularly relevant is the greater stabilization of the highest-energy $\mathbf{TS_{v\text{-}viii}}$, about 15 kcal mol^{-1} in CH_3CN, which translates into a reduction in activation energy of 8.3 kcal mol^{-1} for PMe_3 and 10.3 for $AsMe_3$. When comparing the alternative ligand and solvent-assisted substitution paths after coordination of the alkenyl stannane, it is clearly seen that the latter is kinetically favored. The greater electrophilicity of **iv** relative to **vii** manifests itself on the substantial lowering of the activation energy (*ca.* 10 kcal mol^{-1}). Even though solvent reduces the barrier for the latter to 26.9 kcal mol^{-1} ($\mathbf{TS_{vii\text{-}v}}$) the value is more than 5 kcal mol^{-1} higher than that of the kinetically significant rate-limiting step involving the solvato complex (i.e., $\mathbf{TS_{v\text{-}viii}}$ relative to **iv**). Last, intermediate **viii** dissociates trimethyltin bromide **4**, affording a three-coordinate (T-shaped) palladium complex $PdL(vinyl)_2$ **ix** stabilized by 4.5 kcal mol^{-1} for L = PMe_3 (5.0 kcal mol^{-1} for L = $AsMe_3$).

From the *cis*-Square Planar Complex (*cis*-PdL_2R^1X)

The transmetalation process is usually assumed to take place from the *trans*-square-planar complex (*trans*-PdL_2R^1X). We also considered the pathway that starts from the *cis*-PdL_2R^1X isomer and computed its reaction profile using either L = PH_3 or PMe_3 (Figure 10 and Table 4). Despite their consideration

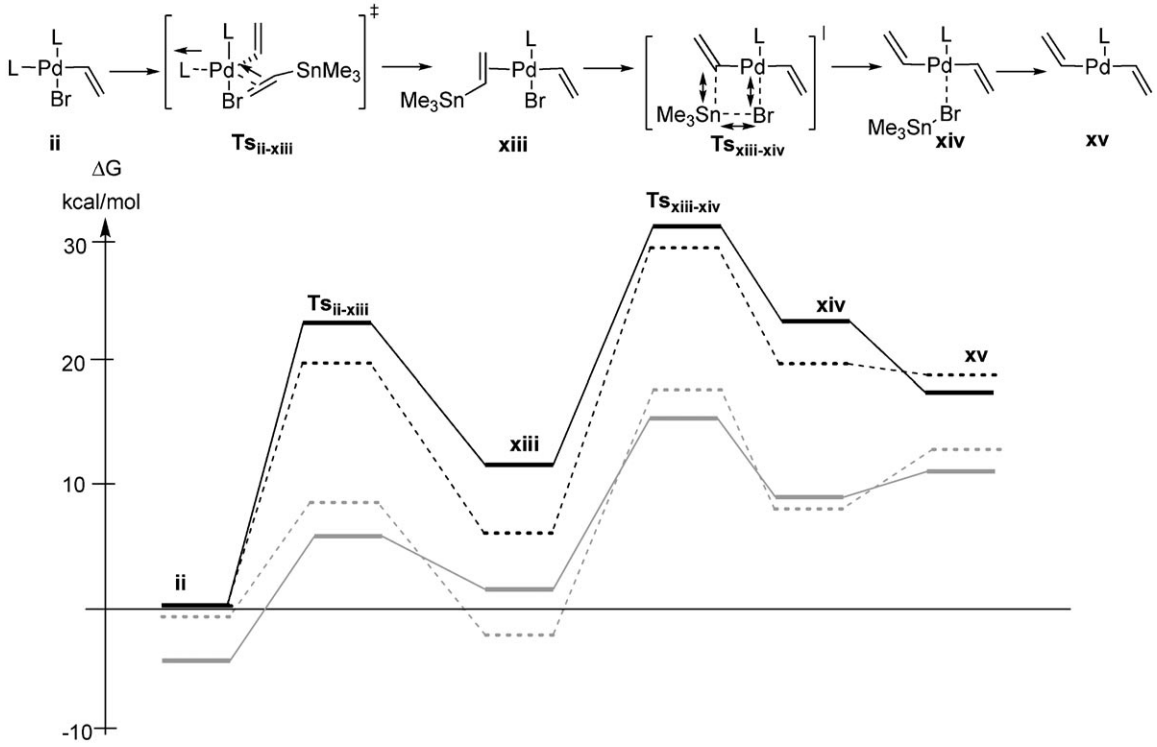

Figure 10. The transmetalation step between **ii** and **xv** (solid line, L = PMe_3; dotted line, L = PH_3; black, gas phase; grey, CH_3CN-COSMO).

Table 4. Gibbs free energies (in kcal mol^{-1}) for the species along the cyclic transmetalation mechanism starting from *cis*-PdL$_2$(vinyl)Br **ii** (L = PMe$_3$ or PH$_3$) and depicted in Figure 10.

Structure	L = PMe$_3$			L = PH$_3$		
	$\Delta G^{[a]}$	$\Delta G^{[b]}$	$\Delta G^{[c]}$	$\Delta G^{[a]}$	$\Delta G^{[b]}$	$\Delta G^{[c]}$
ii	0.0	−4.9	−0.4	0.0	−0.7	2.5
TS$_{ii\text{-}xiii}$	23.7	5.3	11.1	19.9	8.0	12.7
xiii	11.9	1.4	6.1	5.6	−2.1	2.0
TS$_{xiii\text{-}xiv}$	31.1	16.6	21.3	29.3	18.1	22.2
xiv	23.7	9.8	14.7	19.9	8.5	12.7
xv	18.8	11.0	14.3	18.6	13.3	16.0

[a] Gas phase.
[b] CH_3CN (COSMO).
[c] THF (COSMO).

as kinetically irrelevant intermediates except for bidentate phosphines, *cis* complexes have been experimentally characterized.[21]

The transmetalation mechanism starting from *cis*-PdL$_2$(vinyl)Br involves an 18-e$^-$ trigonal bipyramidal complex in which the apical positions are occupied by the donor ligand (PMe$_3$ or PH$_3$) and the bromide.[31] Only a complex with trigonal bipyramidal geometry could be located as a transition state connecting **ii** and **xiii** (L = PMe$_3$ or PH$_3$), the square-planar species with the vinyl groups in *trans* (one of them η^2-coordinated, Figure 10). Coordination of stannane involves ligand dissociation in an endergonic process (**ii** is 5.6 kcal mol^{-1} more stable than **xiii** for PH$_3$; 11.9 kcal mol^{-1} for L = PMe$_3$) and with an energy cost of 23.7 kcal mol^{-1} for PMe$_3$ (19.9 kcal mol^{-1} for L = PH$_3$) to reach **TS$_{ii\text{-}xiii}$** (Figure 7). A cyclic four-coordinate transition state **TS$_{xiii\text{-}xiv}$** (Figure 9) was also found further uphill (energy cost from **xiii** of 19.2 kcal mol^{-1} for L = PMe$_3$ and 23.6 kcal mol^{-1} for L = PH$_3$) which exhibited Br–Pd, Br–Sn and C–SnMe$_3$ bond distances of 2.62, 2.80 and 3.31 Å for PMe$_3$ ligand (2.60, 2.81 and 3.41 Å for PH$_3$ ligand). These values are close to those of transition state **TS$_{v\text{-}viii}$** (2.71, 2.79 and 3.23 Å for the same distances of complex with PMe$_3$) located starting from the *trans*-complex (Figure 9). From **TS$_{xiii\text{-}xiv}$** onwards energy is released (14.2 kcal mol^{-1} for PH$_3$; 11.8 kcal mol^{-1} for PMe$_3$) but the overall transformation from the *cis* intermediate is endergonic: the energy difference between **ii** and **xiv** is 23.7 kcal mol^{-1}, and the energy of activation for transmetalation of *cis*-Pd(PMe$_3$)$_2$(vinyl)Br complex **ii** is 31.1 kcal mol^{-1} (19.9 kcal mol^{-1} and 29.3 kcal mol^{-1} are the corresponding values for PH$_3$). Intermediate **xiv** is characterized by the *trans* arrangement of vinyl groups and the weakening of the Pd–Br bond (P–Br distance of 2.71 Å for the PMe$_3$ complex) as a prelude to forming a three-coordinate palladium complex **xv**. The higher donicity of PMe$_3$ relative to PH$_3$ as shown by their lone pair orbital energies (−8.91 eV for PMe$_3$ and −10.54 eV for PH$_3$; Kohn–Sham orbital energies; B3LYP/6-31G*) together with steric differences might explain the results obtained in the computations for both phosphine models.[32]

All species with incipient charge separation (both transition states and dissociating intermediate **xiv**) are highly stabilized by polar solvent molecules relative to the square-planar complexes **ii** and **xiv**. This in turn considerably reduces the activation energies for the overall transformation by as much as 10 kcal mol^{-1}. The energy of activation in acetonitrile solution for the two-step transmetalation mechanism starting from **ii** is 21.5 kcal mol^{-1} for *cis*-Pd(PMe$_3$)$_2$(vinyl)Br and 18.8 kcal mol^{-1} for *cis*-Pd(PH$_3$)$_2$(vinyl)Br. The energy cost to reach the cyclic transition state **TS$_{v\text{-}viii}$** of the *trans*-Pd(PMe$_3$)$_2$(vinyl)Br catalytic cycle starting from the lowest energy intermediate **vii** (Figure 8) is 30.4 kcal mol^{-1}. This is 8.9 kcal mol^{-1} higher than that of **TS$_{xiii\text{-}xiv}$** relative to **ii** in the same solvent for the alternative *cis*-Pd(PMe$_3$)$_2$(vinyl)Br catalytic cycle. Judging from these values, we concluded that, at least for PMe$_3$, the transmetalation of *cis*-Pd(PMe$_3$)$_2$(vinyl)Br **ii** is favored over that of the *trans*-Pd(PMe$_3$)$_2$(vinyl)Br isomer **vii**.

Isomerization of Tricoordinate Complexes

Transmetalations from both the *trans*- and the *cis*-Pd(L)(Y)(vinyl)Br complexes afford, through the cyclic transmetalation mechanism, three-coordinate Pd(II) complexes **ix** and **xv** (Figure 11). A recent report by Yamashita and Hartwig proves the existence of certain monomeric three-coordinate arylpalladium amido complexes with a single (bulky) phosphine ligand, and several of them were shown by X-ray crystallography to display a T-shaped geometry.[33] This geometric arrangement is also found in complexes **ix** and **xv**, formed upon release of BrSnMe$_3$ from precursors **viii** and **xiv**, but the vinyl groups are *trans* in the latter. Yamashita and Hartwig[34] reported the irreversible reductive elimination of the arylamido product [in contrast to the reversible nature of the reductive elimination from P(*t*-Bu)$_3$Pd(Ar)(X)[33]] from these T complexes but obviously no structural and mechanistic details are avalaible for the irreversible processes. Early theoretical[35] studies on the reductive elimination of d^8 metal complexes confirmed the experimental findings that *trans*-dialkyl-Pd complexes are quite stable and instead of reductive elimination they often undergo β-elimination whenever possible. Should reductive elimination occur, it would take place through the corresponding T-*cis* complexes. Without the intervention of polar coordinating solvents or ligands assisting the isomerization mechanism as suggested,[35] or complex intermolecular ex-

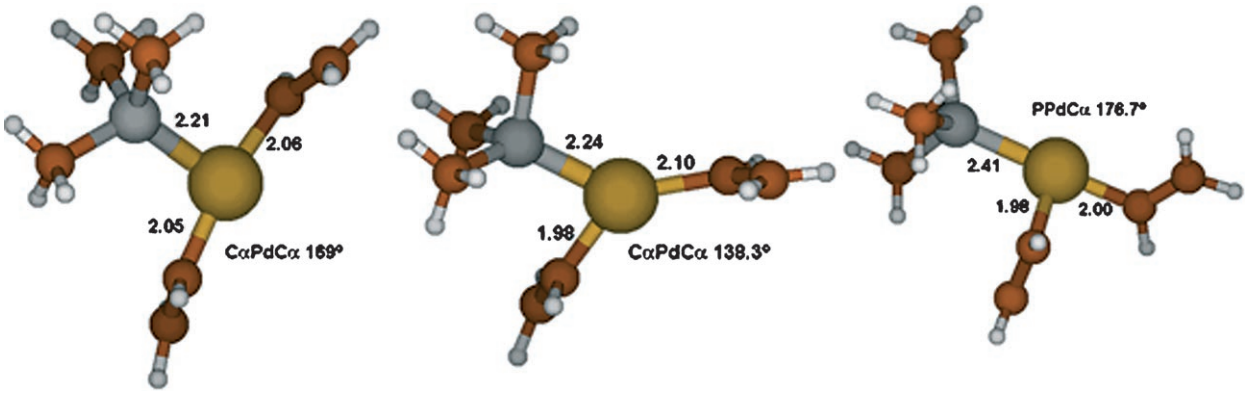

Figure 11. Optimized geometries (B3LYP/6-31G*-SDD) for the isomerization between the three-coordinate complexes **xv** and **ix** on route to *s-trans*-butadiene (**xv**, $\mathbf{TS_{xv\text{-}ix}}$ and **ix**).

change processes,[36] we envisioned a polytopal rearrangement of *trans* to *cis* T complexes *via* a Y transition state. These two geometries have been considered more stable than the ideal trigonal planar structure, and the T more stable than the Y.[35] Our computations confirm that these equilibrating geometries are easily attained, and indeed the Y geometry with a PMe_3 ligand is placed 10.5 kcal mol^{-1} above the T geometry **xv** with the vinyl groups in *trans* (for $AsMe_3$), becoming the transition state interconverting both *trans* and *cis* T-shaped structures. Geometric features of **xv** are the P–Pd–Cα and P–Pd–Cα′ bond angles of 98.1 and 92.1°, respectively, and a Pd–P bond distance of 2.20 Å. The Y-shaped $\mathbf{TS_{xv\text{-}ix}}$ (Figure 11) is reached through the movement of a vinyl group towards the empty coordination site that increases the P–Pd–Cα bond angle up to 142.3°, and the slight bending of the other vinyl substituent (to form a 81.6°Cα–Pd–Cα′ bond angle). Structure **ix** is then generated in an exergonic process (Figure 12) and thus both cycles, starting with *trans*- and *cis*-PdL_2RX complexes converge at this step. **ix** is another T-shaped intermediate with the vinyl groups in *cis* and placed almost perpendicular to each other (Cα–Pd–Cα′ angle of 86.4° and Cα–Cα′ distance of 2.74 Å) and the trimethylphosphine ligand in *trans* to one of the Pd–C bonds (Cα–Pd–P

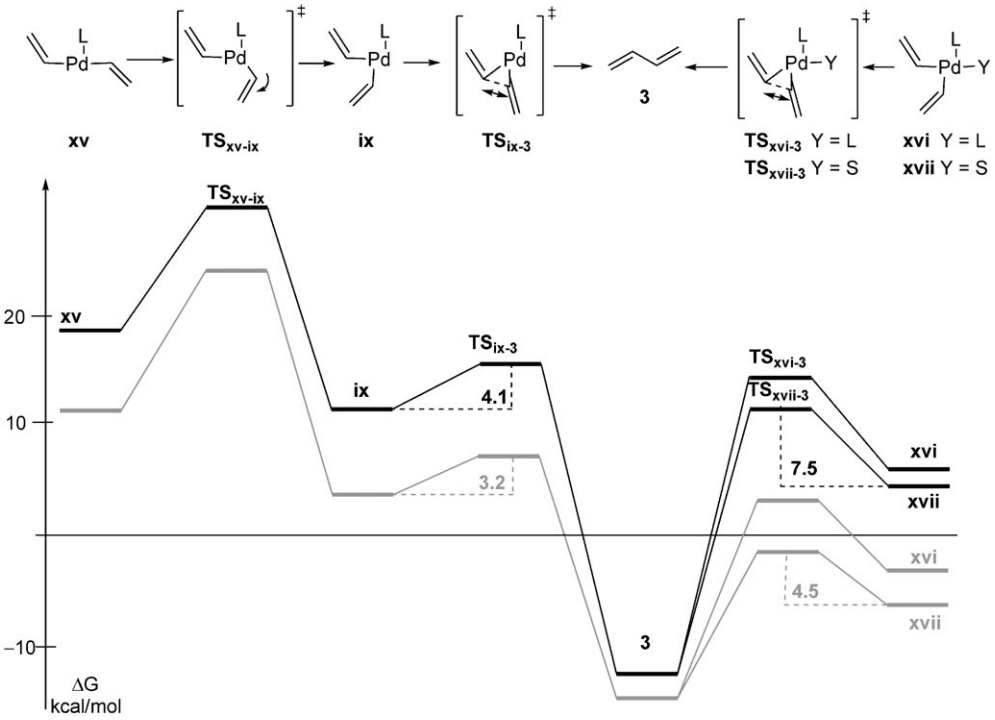

Figure 12. The isomerization and the reductive elimination steps from intermediate $Pd(PMe_3)(vinyl)_2$ **xv** (black, gas phase; grey, CH_3CN-COSMO).

bond angle of 177°). The P–Pd bond length increases to 2.41 Å in $\mathbf{TS_{xv\text{-}ix}}$ (Figure 11) from the original 2.24 Å in **xv** due to the *trans* influence or bond-strength weakening opposite the vinyl ligand (Figure 11).[37]

Reductive Elimination

Three-coordinate *cis*-14 e^- intermediate **ix** (Figure 11) should then undergo fast reductive elimination of the organic fragment (butadiene).[38] A stepwise mechanism (Figure 12) was computationally characterized with a three-center transition state $\mathbf{TS_{ix\text{-}3}}$ (the imaginary frequency corresponds to Cα–Cα′ bond formation of a putative bis-methylidene palladacyclopropane) located uphill that is reached at a low cost (4.1 kcal mol^{-1} for PMe_3; 4.2 kcal mol^{-1} for $AsMe_3$, Table 5), since the internal sp^2/sp^2 carbons are placed at a bond-forming distance of 2.17 Å for both PMe_3 and $AsMe_3$ complexes (Figure 13). This transition structure is achieved by the displacement of the vinyl group located almost perpendicular to the Pd–P bond towards the other (the P–Pd bond distance is reduced to 2.38 Å due to the slight decrease of the *trans* influence on the phosphine ligand) and the Cα–Pd–Cα′ angle reaches 64.8° with Pd–C distances of 2.02 Å. (Figure 12 and Figure 13).[39]

Table 5. Gibbs free energy values (in kcal mol^{-1}) for the species located along the isomerization and the elimination steps depicted in Figure 12 (L = PMe_3).

Structure	ΔG[a]	ΔG[b]	ΔG[c]
xv	18.8	11.0	14.3
$\mathbf{TS_{xv\text{-}ix}}$	29.2	23.6	27.0
ix	11.1	3.5	7.0
$\mathbf{TS_{ix\text{-}3}}$	15.2	6.7	10.2
3	−37.6	−40.3	−38.5
xvi	5.07	−2.6	2.3
$\mathbf{TS_{ix\text{-}3}}$	14.5	3.6	8.4
xvii	4.8	−6.2	−1.6
$\mathbf{TS_{ix-3}}$	12.3	−1.7	2.9

[a] Gas phase.
[b] CH_3CN (COSMO).
[c] THF (COSMO).

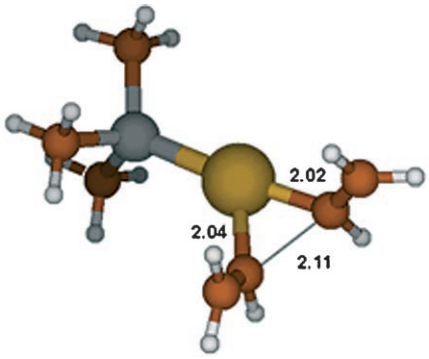

Figure 13. Optimized geometry (B3LYP/6-31G*-SDD) for the transition structure $\mathbf{TS_{ix\text{-}3}}$ of the reductive elimination mechanism to afford s-*trans*-butadiene from **ix**.

Discussion

The efficiency of the Stille cross-coupling is largely dependent upon the judicious (or, oftentimes, empirical) choice of palladium ligands, solvent and additives.[3] Following the seminal work of Stille, Farina et al.[5] first reported the dramatic rate enhancement of low-donicity ligands in a polar coordinating solvent (NMP). Copper salts were also shown to accelerate the reaction, and this discovery was adopted in synthetic sequences.[40] A major breakthrough has been the use of palladium complexes ligated by bulky phosphines, which has particularly impacted synthesis, allowing to fully exploit the number of commercial aryl chlorides as coupling partners to stannanes and related nucleophiles in Pd-catalyzed processes.[41]

Kinetic studies have provided rate equations for Stille coupling reactions that confirmed the rich mechanistic manifold and the complex role of the above mentioned variables.[8,15]

Computational studies can offer alternative views of these transition metal-mediated reactions, supporting some experimental findings or refuting unlikely proposals. We have computationally addressed the effect of Pd ligands (PMe_3, $AsMe_3$ and PH_3) and a coordinating solvent (DMF) in the Stille cross-coupling of vinyl bromide **1** and trimethylvinylstannane **2**. The reaction mechanism has been studied in the gas phase and in a solvent field (CH_3CN and THF with PCM models), and the intermediates and transition states have been fully characterized. Figure 14 and Figure 16 summarize our computationally-based proposal for the Stille reaction between vinyl partners. We describe three alternative Pd-catalyzed cycles starting from *trans*-PdL(DMF)(vinyl)Br **iv**, *trans*-PdL_2(vinyl)Br **vii** and *cis*-PdL_2(vinyl)Br **ii** complexes. A major role for the coordinating solvent has been confirmed, since the activation energy for the highest energy species in the *trans*-PdL(DMF)(vinyl)Br **iv** cycle is the lowest of the three computed, and this is predicted to be the most likely associative mechanism. Figure 16 also compares catalytic cycles for the transmetalation steps originating from the initially formed *cis*-PdL_2(vinyl)Br **ii** and its *trans*-PdL_2(vinyl)Br **vii** isomer, with the former being of lower energy.

The starting palladium complex PdL_2 **i** is converted into the square-planar 16 e^- complex PdL_2(vinyl)Br (L = $AsMe_3$, **ii.As**; L = PMe_3, **ii.P**) by a concerted oxi-

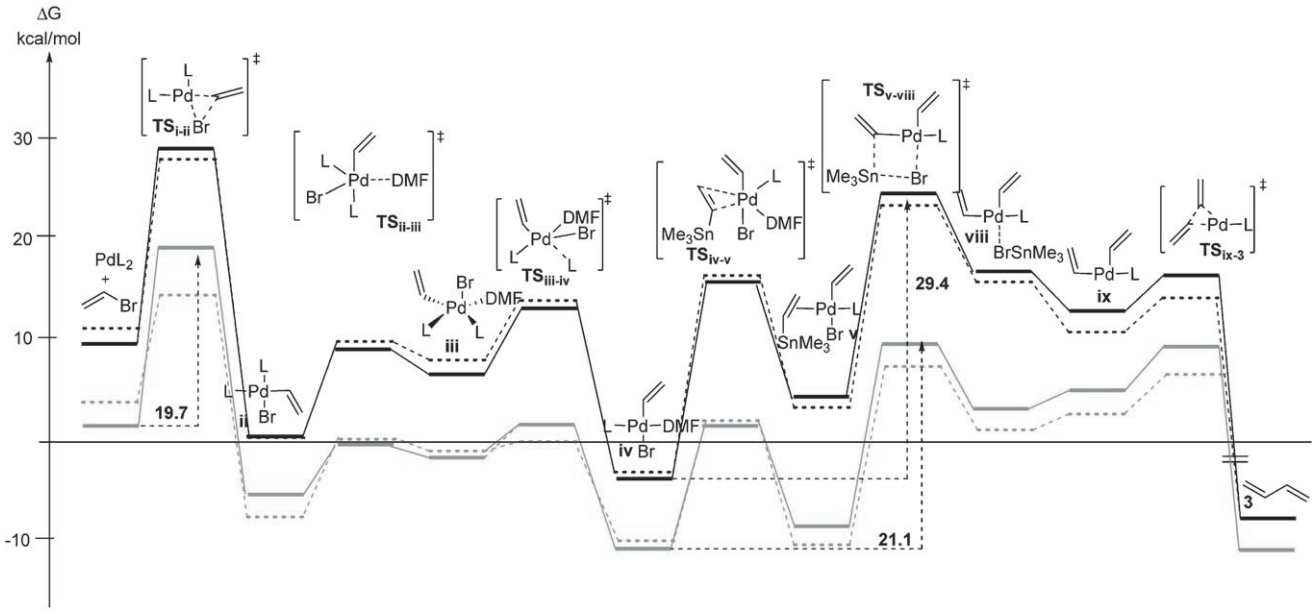

Figure 14. Computed reaction free-energy profile in gas phase (black) and in a solvent field (grey, CH_3CN-COSMO) for the catalytic cycle of the Stille reaction depicted on Figure 3 featuring the transmetalation of the square-planar *trans*-Pd(L)(S)-(vinyl)Br complexes with a coordinating solvent (DMF) (L = PMe_3, solid line; L = $AsMe_3$, dotted line).

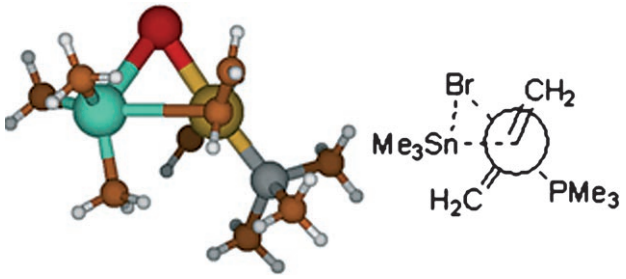

Figure 15. Definition of the puckering (θ) and its application to the cyclic transmetalation transition state $\mathbf{TS_{xiii\text{-}xiv}}$ with PMe_3 as ligand (B3LYP/6-31G*-SDD).

dative addition of vinyl bromide, a step with a large energy barrier (18.9 kcal mol^{-1} for PMe_3; 16.2 kcal mol^{-1} for $AsMe_3$). The energy cost for this pathway is modified in a CH_3CN solvent field (16.6 kcal mol^{-1} for PMe_3; 11.3 kcal mol^{-1} for $AsMe_3$) mostly due to a stabilization of the transition state $\mathbf{TS_{i\text{-}ii}}$, in particular when the ligand is $AsMe_3$. Recently, Norrby et al.[42] determined that the 14 e$^-$ solvato complexes [Pd-(DMF)PPh_3] are more reactive than the phosphino complexes [Pd(PPh_3)$_2$] in the oxidative addition step, which further confirms the need to re-evaluate the nature of the palladium species present in coordinating solvents.

We have incorporated the coordinating solvent at the stage of the *cis-trans* isomerization, inducing the associative substitution of one of the starting ligands. The DMF-assisted isomerization that gives the *trans*-PdL(S)(vinyl)Br complex is less costly in gas phase and virtually independent of the ligand being substituted (PMe_3: 8.0 kcal mol^{-1}; $AsMe_3$: 8.5 kcal mol^{-1}). However the DMF-assisted replacement of an arsine shows a higher barrier in CH_3CN solution than the PMe_3-induced isomerization (5.2 *vs.* 3.9 kcal mol^{-1}). The low values of their activation energies make these isomerization routes highly likely and kinetically irrelevant.

Similar trends in ligand effects are observed during the stannane coordination step, which we found proceeds through ligand dissociation ($\mathbf{TS_{vii\text{-}v}}$) (energy barrier for PMe_3 of 30.4 kcal mol^{-1} and for $AsMe_3$ of 28.0 kcal mol^{-1}). Farina first reported the formation of different species by ligand dissociation, and found that $AsPh_3$ accelerates Stille coupling reactions by a factor of 10^2–10^3.[5] Amatore and Jutand confirmed that $AsPh_3$ accelerates the oxidative addition by a 10-fold factor in DMF compared to PPh_3,[16] but found that this effect is partly canceled out in the presence of the CH_2=CH-Sn(*n*-Bu)$_3$ nucleophile, which interferes in the catalytic cycle prior to the oxidative addition.[15] The greater efficiency of the Stille reaction, when catalyzed by a Pd(0) complex ligated by $AsPh_3$ instead of PPh_3, was alternatively ascribed to a more facile dissociation of $AsPh_3$ from the oxidative addition intermediate Pd($AsPh_3$)$_2$(Ph)I in THF and DMF.[16] We confirmed this assumption in our stannane-assisted ligand (or solvent) dissociation mechanisms in solution and in gas phase, except in the case of the mixed complexes **iii**, for which PMe_3 and $AsMe_3$ release are virtually isoenergetic (20.3 and 20.7 kcal mol^{-1}, respectively).

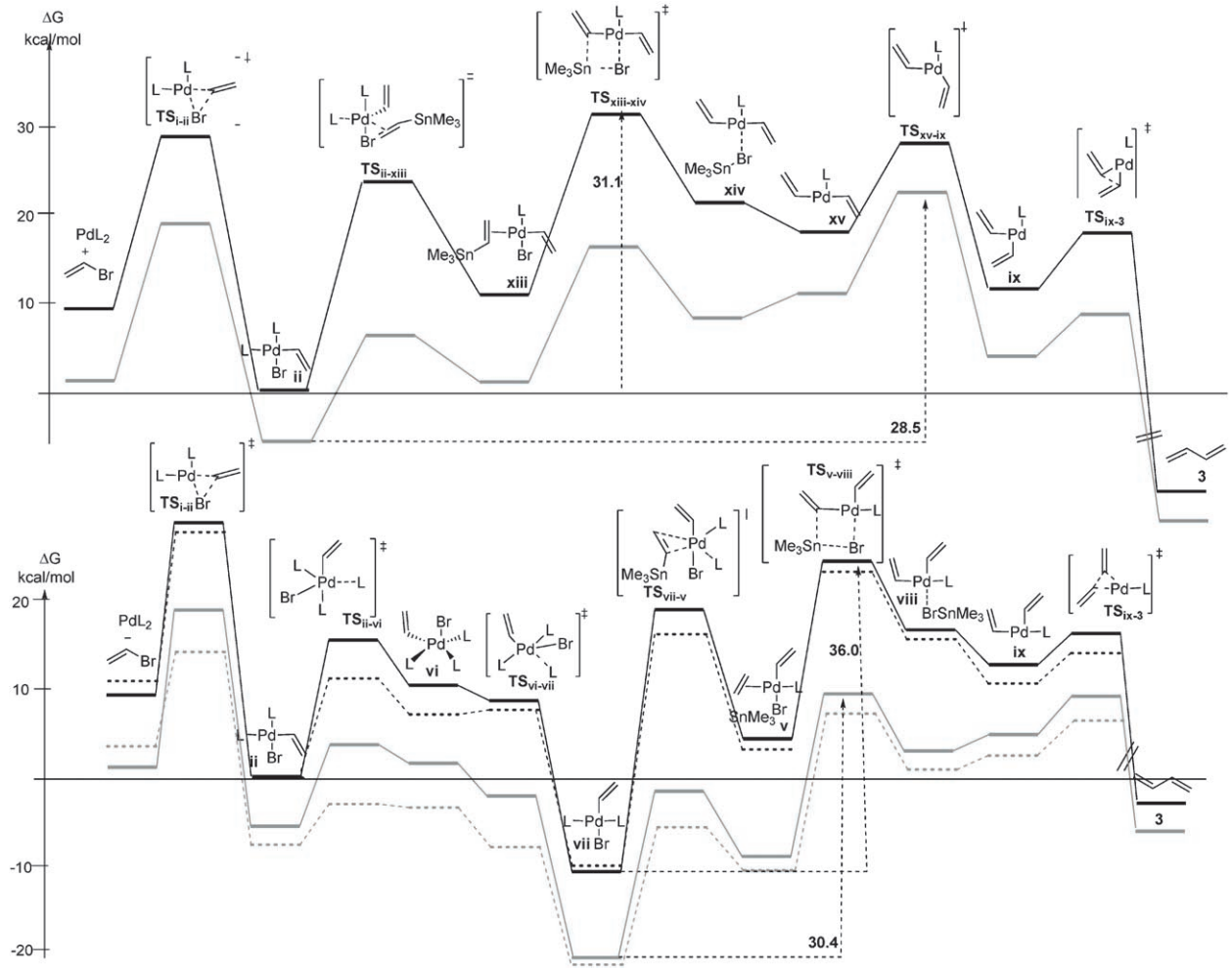

Figure 16. Computed free-energy profiles in gas phase (black) and in solvent (grey, CH_3CN-COSMO) for the *cis*- (top) and *trans*-PdL_2(vinyl)Br (bottom) (L = PMe_3, solid line; L = $AsMe_3$, dotted line) complexes **ii** and **vii**, respectively, in the absence of coordinating solvents.

The same authors later reported that the transmetalation step of the Stille reaction involving CH_2=CH-Sn(*n*-Bu)$_3$ as nucleophile proceeds mainly *via* the 1:1 reaction of the tin derivative with Pd($AsPh_3$)(DMF)(Ph)I formed by the dissociation of one $AsPh_3$ ligand from Pd($AsPh_3$)$_2$(Ph)I. This argument is in agreement with Farina's conclusions for the same reactants and ligands, despite the different experimental conditions (THF, 50 °C).[5] Species Pd($AsPh_3$)(DMF)(Ph)I, undetectable by ^{1}H NMR in the range of $AsPh_3$ concentrations used, was confirmed kinetically as the reactive complex that couples to the stannanes (assuming steady state approximation), in keeping with the efficiency of Stille reactions catalyzed by $AsPh_3$-liganded palladium complexes.[16]

Our computations confirm the greater reactivity of the mixed phosphine or arsine/DMF complexes relative to the analogues with identical ligands (Table 6). Moreover, the Pd(L)(DMF)(vinyl)Br complex **v** is the kinetically competent intermediate, since it is reached after ligand dissociation and before the proper transmetalation step.

The highest energy species in the associative Stille catalytic cycle (Table 6) starting from the *trans*-Pd(L)(Y)(vinyl)Br complexes is the *cyclic four-coordinate* transition state (**TS$_{v\text{-}viii}$**, Figure 15) with a Br ligand bridging Pd and Sn, and the Me_3Sn shifting rapidly between the vinyl and Br groups. These are highly puckered structures, which are not qualitatively modified by the different ligands (PMe_3 or $AsMe_3$) as infered from the values of the arbitralily chosen Br–Pd–C–Sn dihedrals (see Figure 15): 47.8° for **TS$_{v\text{-}viii}$•P** and 50.1° for **TS$_{v\text{-}viii}$•As**. Should a chiral alkyl (benzyl) stannane be used, the coupling through the cyclic four-membered transition state is predicted to proceed with retention of configuration, thus explaining the results of Falck et al.[7] In the case the transition state could be formed by a direct bimolecular reaction

Table 6. Free energy differences (in kcal mol^{-1}) for stannane addition, the formation of the cyclic transmetalation and the overall two-step transmetalation process (gas phase, normal font; CH_3CN solvent field in italics).

Complex	Coordination of stannane $\mathbf{TS_{iv\text{-}v}}$, $\mathbf{TS_{vii\text{-}v}}$ and $\mathbf{TS_{ii\text{-}xiii}}$	Cyclic transmetalation $\mathbf{TS_{v\text{-}viii}}$ and $\mathbf{TS_{xiiixiv}}$	Two-step overall transmetalation $\mathbf{iv–TS_{v\text{-}viii}}$, $\mathbf{vii–TS_{v\text{-}viii}}$, $\mathbf{ii–TS_{xiii\text{-}xiv}}$
trans-PMe_3	30.4	20.4	36.0
	19.0	*18.7*	*30.4*
trans-$AsMe_3$	26.8	20.0	33.3
	14.7	*18.3*	*28.4*
trans-PMe_3/DMF	20.3	20.4	29.4
	12.2	*18.7*	*21.1*
trans-$AsMe_3$/DMF	20.6	20.0	27.5
	10.9	*18.3*	*17.2*
trans-PH_3	17.8	–[a]	–
	9.2	–	–
cis-PMe_3	23.7	19.2	31.1
	10.2	*15.2*	*21.5*
cis-PH_3	19.9	23.7	29.3
	8.7	*20.2*	*18.8*

[a] –: not determined.

of the stannane with the Pd complex, or by formation of a previous coordination complex with the aryl group of the benzyl-stannane reagent.

We have also computed some of the steps for the Stille catalytic cycle using palladium coordinated to the more simplified PH_3 ligand. It has been recognized that changing substituents on phosphine ligands can cause marked changes in the behavior of their transition metal complexes. This ligand capacity has been correlated with the steric effect (cone angle,ϕ) as a result of forces between parts of a molecule and the electronic effect (Tolman parameter, ν)[43] as a result of transmission along the chemical bond. From our computations, PH_3 dissociates more easily than PMe_3 upon ligand substitution by the trimethyl vinylstannane with a kinetic preference of about 12.6 kcal mol^{-1} in gas phase and 10.0 kcal mol^{-1} in solution.

The incorporation of other ligands at the metal, as arsines (AsR_3), which are thermodynamically and kinetically more labile than PR_3, facilitate the formation of intermediates in reactions proceeding *via* ligand dissociation, as our computations confirm.[42]

As shown in Table 6, activation energies from the lowest energy intermediate **iv** going through **v** and reaching $\mathbf{TS_{v\text{-}viii}}$ are smaller for the $AsMe_3$ complex than for the PMe_3 analogue (energy differences of 1.8 kcal mol^{-1} in the gas phase and 3.8 kcal mol^{-1} in CH_3CN as solvent were computed). This difference is consistent with kinetic data based on conductivity measurements in which reactions run in DMF are 670 times faster with $AsPh_3$ than with PPh_3 as palladium ligands.[16]

When the coordinating solvent is not included in the computations, the reaction could eventually proceed through the initially formed *cis*-PdL_2(vinyl)Br **ii** complex or from its isomer *trans*-PdL_2(vinyl)Br **vii**. The latter was conceived to be formed by an associative substitution with excess ligand. The energy barriers for the ligand-assisted isomerization reaction, in gas phase, are 15.4 kcal mol^{-1} for $L=PMe_3$ and 11.8 kcal mol^{-1} for $L=AsMe_3$. In CH_3CN, these are reduced to 9.1 and 3.9 kcal mol^{-1}, respectively, in agreement with the more labile nature of the Pd-As bonds compared to the Pd–P bonds. The overall isomerization step is exergonic, and intermediate **vii**, the most stable of the catalytic cycle, is found 11.3 kcal mol^{-1} below **ii**. From square-planar *trans* complex **vii**, the steps are similar to those of the solvento complex **iv**. Upon ligand substitution, both species converge at intermediate **v** and the same transition state ($\mathbf{TS_{v\text{-}viii}}$) is found. The stability of **vii** increases the activation energy for transmetalation to 36.0 kcal mol^{-1} (6.6 kcal mol^{-1} higher than the same step from the solvento complex **iv**).

The activation energy in gas phase for the transmetalation step that takes place from the palladium complex with *cis* geometry (Figure 16) *cis*-PdL_2(vinyl)Br **ii** is 31.1 kcal mol^{-1}, a value *ca.* 5 kcal mol^{-1} smaller than that starting from *trans*-PdL_2(vinyl)Br **vii** (Figure 16). Both mechanisms evolve through cyclic four-coordinate transition states to afford a T-shaped complex which will need to isomerize and eliminate butadiene, regenerating the Pd(0) catalyst. $\mathbf{TS_{xiii\text{-}xiv}}$ shows a greater puckering (55.5°) than its analogues (see Figure 9), which might be related to the more severe steric interaction of the methyl groups at P and Sn in an already congested environment. The transmetalation step for the *cis* complexes having PH_3 and PMe_3 as ligands also show the easier dissociation of the former, but the differences are smaller than those computed for the L-assisted isomerization. The stannane coordination is the step that shows the greatest energy differ-

ence between PH_3 and PMe_3 along the transmetalation path (3.8 kcal mol^{-1}).

The solvent stabilizes the cyclic transition state to a greater extent than more advanced intermediates along the cycle. This results in activation energies for transmetalation of 30.4 kcal mol^{-1} for the *trans*- and 21.5 kcal mol^{-1} for the *cis* isomer in CH_3CN. Interestingly, the smaller stabilization of the transition state for isomerization of the T complexes $\mathbf{TS_{xv\text{-}ix}}$ in solution makes this the highest energy species of the *cis*-cycle (28.5 kcal mol^{-1} from **ii** with PMe_3 as ligand). In consequence, *cis*-Pd(PMe_3)$_2$(vinyl)Br **ii** will become the kinetically relevant species in the absence of coordinating solvent molecules. Therefore, although in most cases the *trans* oxidative addition complex has been the only isolated species (in accordance with its thermodynamic stability), the *cis* isomers might be driving the Stille coupling under certain experimental conditions (i.e., when a non-coordinating solvent ligand is used). One can only speculate at this stage about the effects of excess phosphine on the Stille reactions, but judging from our computations, solvent could induce the *cis*-Pd(PMe_3)$_2$(vinyl)Br **ii** to the *trans*-Pd(PMe_3)$_2$(vinyl)Br **vii** isomerization leading to species that are significantly more stable (e.g., **vii**) and increase accordingly the activation barriers for the rate-limiting transmetalation, thus retarding the entire catalytic cycle.

The isomerization between the T-shaped three-coordinate complexes to bring the *trans* vinyl ligands closer and placed at a perpendicular geometry is feasible through Y-shaped transition states. We have computed the energy profiles for the two discrete orientation of the vinyl groups bound to Pd, the equivalent s-*trans* or s-*cis* conformations of the final butadiene. In both cases (only the formation of s-*trans*-butadiene is shown here),[39] the species found along the potential energy surface show similar energies and geometries. First, one of the vinyl substituents bends over the empty coordination site left vacant by the release of $BrSnMe_3$, to additionally stabilize the complexes at product **ix** by the reduction in steric congestion. This movement of the vinyl group is the more costly step in the isomerization and reductive elimination steps, since it requires around 10.5 kcal mol^{-1}.

Once the vinyl ligands occupy the perpendicular position in a T-shape intermediate, reductive elimination[44] ensues. Recent computational studies have focused on reductive elimination of dienes from unsaturated vinyl units bound to transition metal complexes.[45] Tetracoordinated metal complexes with two halogens or donating groups (PH_3, NH_3) and the vinyl ligands in mutual *cis* relationships were chosen as models. The activation energies corresponding to the Cα–Cα' bond formation on the Pd(PH_3)$_2$(vinyl)$_2$ complex is 6.8 kcal mol^{-1}, corresponding to an early transition state with the forming C–C distance of 2.02 Å and the Cα–Pd–Cα' angle of 58.4°.[45] Although the vinyl groups of our *cis*-three-centered complexes **ix** are placed at the same bond-forming distance than in the tetracoordinated complexes (2.02 Å), the internal Cα–Pd–Cα' angle is larger, 64.8 Å, most likely due to the reduced steric interaction in three- *vs.* the four-coordinate complexes, which is also reflected on the lower activation energy for the bond-forming event from the three-coordinate complexes (4.0 kcal mol^{-1}).

A considerably exergonic reaction from $\mathbf{TS_{ix\text{-}3}}$ (about 40 kcal mol^{-1}) is associated with the C–C bond formation and further stabilization of the conjugated diene **3** in its s-*trans* or s-*cis* conformation from the T complex **ix**.

Conclusions

Recent experimental findings support a complex mechanistic manifold for the Stille reaction in which the nature of the palladium ligands, the leaving group and the solvent (not to mention the additives) play fundamental roles driving the reactions through associative or dissociative mechanisms. The nature of the species implicated and the effect of the reaction variables in their structure and energy content is also subject to debate. A computational study was therefore conducted in order to support some of these proposals. We have chosen as model system the formation of butadiene through the coupling of vinyl bromide **1** and trimethylvinylstannane **2** by the most likely associative transmetalation mechanism. Our findings can be summarized as follows: a) the associative mechanism involves a high energy puckered cyclic transition state linking Pd, Br, Sn and sp^2 C atoms that eliminates Br–$SnMe_3$ affording a T-shaped intermediate which proceeds towards reductive elimination; b) this cyclic transition state can be reached either from the *trans*-PdL(Y)(vinyl)Br **iv** or **vii** or from the *cis*-PdL_2(vinyl)Br **ii** oxidative addition product, the latter formed from PdL_2 and vinyl bromide **1** by a concerted insertion process; c) analysis of the potential energy surface reveals that the *trans*-PdL(DMF)(vinyl)Br **iv** complex (L = PMe_3 or $AsMe_3$) having a coordinating solvent ligand is the kinetic relevant species, and the solvent contributes to lower the activation energy of the rate-determining transmetalation step; d) the solvent can enter the palladium coordination sphere assisting topomerization of *cis*-PdL_2(vinyl)Br **ii** to *trans*-PdL(Y)(vinyl)Br (Y = PMe_3 **vii** or DMF **iv**) complexes *via* pentacoordinated Pd species; e) the Stille reactions run in DMF (or the most common NMP) through Pd(L)(DMF)(vinyl)Br complexes **iv** are much faster using $AsMe_3$ rather than PMe_3 as palladium ligands; f) in the absence of the coordinating solvent, our computations predict that the Stille reaction of *cis*-PdL_2(vinyl)Br **ii** is favored over that of the

trans-PdL_2(vinyl)Br isomer **vii**; g) a possible explanation (not discarding their effects on stabilizing the T complexes) to the retarding effect of phosphine ligands on Stille reactions rests on the ligand-assisted *cis*-$Pd(PMe_3)_2$(vinyl)Br **ii** to *trans*-$Pd(PMe_3)_2$(vinyl)Br **vii** isomerization, diverting the transition metal into a catalytic cycle that is energetically penalized due to the stability of **vii**; h) the polytopal rearrangements *via* a Y-shaped isomer interconvert the T-shaped three-coordinate complexes formed after the cyclic transmetalation step; i) this Y-shaped structure becomes the highest energy species along the catalytic cycle of the Stille coupling of *cis*-$Pd(PMe_3)_2$(vinyl)Br **ii** in CH_3CN; j) the T-shaped complex with the vinyl ligands in *cis* further distort to another Y-shaped transition state to favor vinyl-vinyl bond formation.

Experimental Section

Computational Methods

All computations in this study have been performed using the Gaussian03 suite of programs.[46] To include electron correlation at a reasonable computational cost, density functional theory (DFT) was used. The Becke three-parameter exchange functional and the nonlocal correlation functional of Lee, Yang, and Parr (B3LYP)[47] with the 6–31G*[48] set for C, H and P, in conjunction with the Stuttgart/Dresden relativistic effective core potentials for Pd, Sn and Br were used to compute the geometries, energies, and normal mode vibration frequencies of the starting material, the corresponding transition structures, and the products. No symmetry constraints were imposed during structural optimizations. The stationary points were characterized by means of harmonic analysis, and for all the transition structures, the vibration related to the imaginary frequency corresponds to the nuclear motion along the reaction coordinate under study. The effect of the solvent (THF and CH_3CN) was taken into account for some of the systems under study through single point calculations at each optimized geometry using the polarized-continuum-model (PCM) at 298.15 K.[49]

Supporting Information

File containing Cartesian coordinates and total energy for all computed structures.

Acknowledgements

We are grateful to the European Community (EPITRON, LSHC-CT-2005-518417) and MEC (SAF2004–07131, FEDER) for financial support. The authors thank the Centro de Supercomputación de Galicia (CESGA) and the Centro de Computación Científica (UAM) for computational resources.

References

[1] a) F. Diederich, P. J. Stang, *Metal-catalyzed Cross-coupling Reactions*, Wiley-VCH, Weinheim, **1997**; b) A. de Meijere, F. Diederich, *Metal-catalyzed Cross-coupling Reactions*, Wiley-VCH, Weinheim, **2004**.

[2] K. C. Nicolaou, P. G. Bulger; D. Sarlah, *Angew. Chem. Int. Ed.* **2005**, *44*, 4442.

[3] P. Espinet; A. M. Echavarren, *Angew. Chem. Int. Ed.* **2004**, *43*, 4704.

[4] a) S. Niu, M. B. Hall, *Chem. Rev.* **2000**, *100*, 353; b) V. P. Ananikov, D. G. Musaev, K. Morokuma, *J. Am. Chem. Soc.* **2002**, *124*, 2839; c) T. Matsubara, *Organometallics* **2003**, *22*, 4286.

[5] a) V. Farina, B. Krishnan, *J. Am. Chem. Soc.* **1991**, *113*, 9585; b) V. Farina, G. P. Roth, *Recent Advances in the Stille Reaction*, in: *Advances in Metal-Organic Chemistry*, (Ed.: L. Liebeskind), JAI Press, **1996**, Volume 5, pp. 1–53.

[6] J. W. Labadie, J. K. Stille, *J. Am. Chem. Soc.* **1983**, *105*, 6129.

[7] J. Ye; R. K. Bath, J. R. Falck, *J. Am. Chem. Soc.* **1994**, *116*, 1.

[8] a) A. L. Casado, P. Espinet, *J. Am. Chem. Soc.* **1998**, *120*, 8978; b) A. L. Casado, P. J. Espinet, A. M. Gallego, *J. Am. Chem. Soc.* **2000**, *122*, 11771; c) J. A. Casares, P. Espinet, G. Salas, *Chem. Eur. J.* **2002**, *8*, 4844.

[9] a) A. C. Braga, G. Ujaque, F. Maseras, *Organometallics* **2006**, *25*, 3647; b) A. C. Braga, N. H. Morgon, G. Ujaque, A. Lledos, F. Maseras, *J. Organometallics Chem.* **2006**, *691*, 4459; c) A. C. Braga, N. H. Morgon, G. Ujaque, F. Maseras, *J. Am. Chem. Soc.* **2005**, *127*, 9298.

[10] M. Sumimoto, N. Iwane, T. Takahama, S. Sasaki, *J. Am. Chem. Soc.* **2004**, *126*, 10457.

[11] a) L. J. Goossen, D. Koley, H. Hermann, W. Thiel, *J. Am. Chem. Soc.* **2005**, *127*, 11102; b) L. J. Goossen, D. Koley, H. Hermann, W. Thiel, *Organometallics* **2006**, *25*, 54.

[12] a) M. Méndez, J. M. Cuerva, D. J. Cárdenas, A. M. Echavarren, *Chem. Eur. J.* **2002**, *8*, 3620; b) O. Nieto-Faza, C. Silva-López, R. Álvarez, A. R. de Lera, *J. Am. Chem. Soc.* **2006**, *128*, 2434.

[13] a) R. Alvarez, O. Nieto-Faza, C. Silva-López, A. R. de Lera, *Org. Lett.* **2006**, *8*, 35; b) for a recent computational study of the competitive associative and dissociative mechanism, see: A. Nova, G. Ujaque, F. Maseras, A. Lledos, P. J. Espinet, *J. Am Chem. Soc.*, **2006**, *128*, 14571.

[14] a) R. G. Parr, W. Yang, *Density Functional Theory of Atoms and Molecules*, Oxford University Press, New York, **1989**; b) T. Ziegler, *Chem. Rev.* **1991**, *91*, 651; c) C. Lee, W. Yang, R. G. Parr, *Phys. Rev. B* **1988**, *37*, 785; d) for a description of density functionals as implemented in the Gaussian series of programs, see: B. G. Johnson, P. M. W. Gill, J. A. Pople, *J. Chem. Phys.* **1993**, *98*, 5612.

[15] C. Amatore, A. Bacaille, A. Fuxa, A. Jutand, G. Meyer, A. Ndedi Ntepe *Chem. Eur. J.* **2001**, *7*, 2134.

[16] C. Amatore A. A. Bahsoun, A. Jutand, G. Meyer, A. Ndedi Ntepe, L. Ricard, *J. Am. Chem. Soc.* **2003**, *125*, 4212.

[17] a) H. Urata, M. Tanaka, T. Fuchikami, *Chem. Lett.* **1987**, 751; b) H. Urata, H. Suzuki, Y. Morooka, T. Ikawa, *J. Organomet. Chem.* **1989**, *364*, 235; c) A. Fürstner, G. Seidel, D. Kremzow, C. W. Lehmann, *Organometallics* **2003**, *22*, 907; d) T. Aoki, Y. Ishii, Y. Mizobe, M. Hidai, *Chem. Lett.* **1991**, 615; e) J.-F. Carpentier, Y. Castaner, J. Brocard, A. Mortreux, F. Rose-Munch, C. Susanne, E. Rose, *J. Organomet. Chem.* **1995**, *493*, C22.

[18] a) L. J. Goossen, D. Koley, H. Hermann, W. Thiel, *Chem. Commun.* **2004**, 2141; b) M. H. Senn, T. Ziegler, *Organometallics* **2004**, *23*, 2980; c) L. J. Goossen, D. Koley, H. Hermann, W. Thiel, *Organometallics* **2005**, *24*, 2398; d) L. J. Goossen, D. Koley;, H. Hermann, W. Thiel, *Organometallics* **2006**, *25*, 54; e) S. Kozuch, S. Shaik, *J. Am. Chem. Soc.* **2006**, *128*, 3355; f) M. Ahlquist, S. Kozuch, S. Shaik, D. Tanner, P.-O. Norrby, *Organometallics* **2006**, *25*, 45.

[19] The coordination of vinylbromide to PdL_2 to form a vinyl complex prior to the oxidative addition was also computed. Although feasible, this step does not substantially modify the energetics of the oxidative addition step.

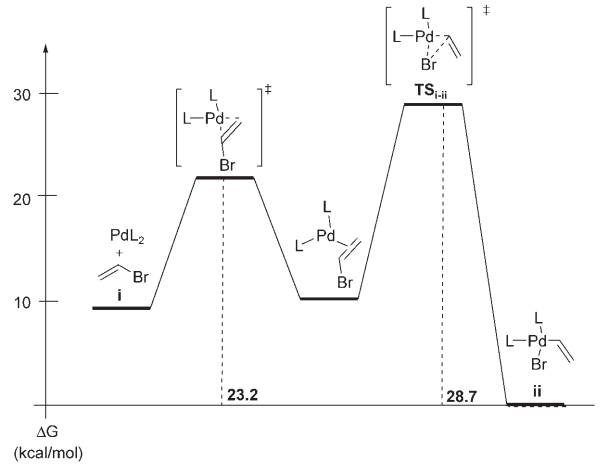

[20] A. L. Casado, P. Espinet, *Organometallics* **1998**, *17*, 954.

[21] H. Urata, M. Tanaka, T. Fuchikami, *Chem. Lett.* **1987**, 751.

[22] F. Basolo, G. Pearson, *Mechanisms of Inorganic Reactions*, 2nd edn., Wiley, New York, **1967**.

[23] R. S. Berry, *J. Chem. Phys.* **1960**, *32*, 933.

[24] R. S. Pavoneas, W. C. Trogler, *J. Am. Chem. Soc.* **1982**, *104*, 3529.

[25] C. S. Lopez, O. N. Faza, A. R. de Lera, D. M. York, *Chem: Eur. J.* **2005**, *11*, 2081.

[26] J. Albanese-Walker, C. Bazaral, T. Leavey, P. G. Dormer, J. A. Murry, *Org. Lett.* **2004**, *6*, 2097.

[27] The high *trans* influence of the carbon ligands (*transphobia*)on phosphines destabilizes these complexes, see: J. Vicente, A. Arcar, D. Bautista, P. G. Jones, *Organometallics* **1997**, *16*, 2127.

[28] Musco et al. have studied the dissociation equilibria of ligand at Pd (PdL_4–PdL_3–PdL_2) and found that the extent of L dissociation is dominated by steric effects, see: a) A. Musco; W. Kuran, A. Silvani, W. Ander, *J. Chem. Soc., Chem. Commun.* **1973**, 938; b) W. Kuran, A. Musco, *Inorg. Chim. Acta* **1975**, 187; c) B. E. Mann, A. Musco, *J. Chem. Soc., Dalton Trans: Inorg. Chem.* **1975**, 753.

[29] Bipyramidal transition states with Pd included in a five-membered ring have been recently found in the context of Pd-Pd transmetalations, see: D. J. Cárdenas, B. Martín-Matute, A. M. Echavarren, *J. Am. Chem. Soc.* **2006**, *128*, 5033.

[30] E. Napolitano, V. Farina, M. Persico, *Organometallics* **2003**, *22*, 4030.

[31] We also considered the transmetalation involving the isomeric bipyramid in which the apical positions are occupied by a ligand and the vinyl group. This process generates the complex **xii**, which is unable to eliminate trimethyltin bromide **4**, since both ligands are placed in *trans.* Cartesian coordinates and energies of the computed structures for this mechanistic variant are provided in the Supporting Information.

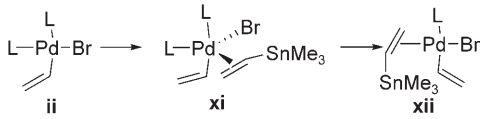

[32] Y. Ohnishi, T. Matsunaga, Y. Nakao, H. Sato, S. Sakaki, *J. Am. Chem. Soc.* **2005**, *127*, 4021.

[33] M. Yamashita, J. F. Hartwig, *J. Am. Chem. Soc.* **2004**, *126*, 5344.

[34] A. H. Roy, J. F. Hartwig, *J. Am. Chem. Soc.* **2003**, *125*, 13944.

[35] K. Tatsumi, R. Hoffmann, A. Yamamoto, J. K. Stille, *Bull. Chem. Soc. Jpn.* **1981**, *54*, 1857.

[36] F. Ozawa, M. Fujimori, T. Yamamoto, A. Yamamoto, *Organometallics* **1986**, *5*, 2149.

[37] R. H. Crabtee, *The Organometallic Chemistry of the Transition Metals*, Wiley-VCH, Hoboken, NJ, **2005**, pp 6–7 and 109–110.

[38] J. M. Brown, N. A. Cooley, *Chem. Rev.* **1988**, *88*, 1031.

[39] Given the presumably easy isomerization of the starting T-shaped Pd complex **xv** to an isomeric one labeled **xviii** (the energy difference between them is negligible, a mere 0.8 kcal mol^{-1}) in which both vinyl groups are placed in *cis* orientation, we also computed the energy profile corresponding to the three-coordinate T to T polytopal rearrangement that converts **xviii** to **xix** via the Y-shaped transition state and the ensuing reductive elimination to form s-*cis*-butadiene. Structures are similar to those presented above for s-*trans*-butadiene (see Supporting Information for details)..

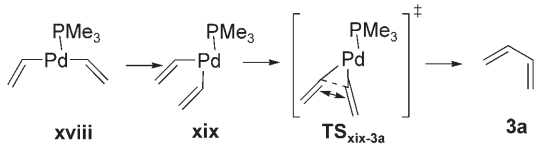

[40] a) L. Liebeskind, R. W. Fengl, *J. Org. Chem.* **1990**, *55*, 5359; b) V. Farina, S. Kapadia, B. Krishnan, C. Wang, L. Liebeskind, *J. Org. Chem.* **1994**, *59*, 5905.

[41] See, for example: A. F. Littke, L. Schwarz, G. C. Fu, *J. Am. Chem. Soc.* **2002**, *124*, 6343.

[42] M. Ahlquist, P. Fristrup, D. Tanner, P.-O. Norrby, *Organometallics* **2006**, *25*, 2066.
[43] C. A. Tolman, *Chem. Rev.* **1977**, *77*, 313.
[44] F. Ozawa, *Reductive Elimination*, in: *Current Methods in Inorganic Chemistry*, Vol. 3, (Eds.: H. Kurosawa, A. Yamamoto), Elsevier, **2003**, chapter 9, pp. 479–511.
[45] a) V. P. Ananikov, D. G. Musaev, K. Morokuma, *J. Am. Chem. Soc.* **2002**, *124*, 2839; b) V. P. Ananikov, D. G. Musaev, K. Morokuma, *Organometallics* **2005**, *24*, 715.
[46] M. J. Frisch, G. W. Trucks, H. B. Schlegel, G. E. Scuseria, M. A. Robb; J. R. Cheeseman, J. A. Montgomery, Jr., T. Vreven, K. N. Kudin, J. C. Burant, J. M. Millam, S. S. Iyengar, J. Tomasi, V. Barone, B. Mennucci, M. Cossi, G. Scalmani, N. Rega, G. A. Petersson, H. Nakatsuji, M. Hada, M. Ehara, K. Toyota, R. Fukuda, J. Hasegawa, M. Ishida, T. Nakajima, Y. Honda, O. Kitao, H. Nakai, M. Klene, X. Li, J. E. Knox, H. P. Hratchian, J. B. Cross, V. Bakken, C. Adamo, J. Jaramillo, R. Gomperts, R. E. Stratmann, O. Yazyev, A. J. Austin, R. Cammi, C. Pomelli, J. W. Ochterski, P. Y. Ayala, K. Morokuma, G. A. Voth, P. Salvador, J. J. Dannenberg, V. G. Zakrzewski, S. Dapprich, A. D. Daniels, M. C. Strain, O. Farkas, D. K. Malick, A. D. Rabuck, K. Raghavachari, J. B. Foresman, J. V. Ortiz, Q. Cui, A. G. Baboul, S. Clifford, J. Cioslowski, B. B. Stefanov, G. Liu, A. Liashenko, P. Piskorz, I. Komaromi, R. L. Martin, D. J. Fox, T. Keith, M. A. Al-Laham, C. Y. Peng, A. Nanayakkara, M. Challacombe, P. M. W. Gill, B. Johnson, W. Chen, M. W. Wong, C. Gonzalez, J. A. Pople, *Gaussian 03, Revision C.02,* Gaussian, Inc., Wallingford CT, **2004**.
[47] a) R. G. Parr, W. Yang, *Density Functional Theory of Atoms and Molecules*, Oxford, New York, **1989**; b) T. Ziegler, *Chem. Rev.* **1991**, *91*, 651; c) C. Lee, W. Yang, R. G. Parr, *Phys. Rev. B* **1988**, *37*, 785.
[48] We have computed some of the relevant steps using 6–311G*/SDD as basis set, with a triple-zeta quality set for all atoms. We found that the geometries of the species and the ΔG values were comparable to those of the smaller 6–31G*/SDD, basis set despite the considerable penalty in computational time (*ca.* three-fold).
[49] a) J. Tomasi, M. Persico, *Chem. Rev.* **1994**, *94*, 2027; b) J. Tomasi, B. Mennucci, R. Cammi, *Chem. Rev* **2005**, *105*, 2999.

